UNIVERSIDADE DA CORUÑA

ORGANIZACIÓN LATINOAMERICANA DE ENERGÍA

SICREEE Centro Regional de Energía Renovable y Eficiencia Energética

SICA Sistema de la Integración Centroamericana

Máster Univ en Eficiencia Energética y Sostenibilidad

José Luis Calvo Rolle

Optimizing bioclimatic houses with intelligent systems

Grupo de Investigación Ciencia y Técnica Cibernética

July 27th, 2022

Table of contents

Basic information

- Research group name: Cybernetic Science and Technique (CTC).

General data

Coordinator	Dr. José Luis Calvo Rolle
Date of birth	10/05/2005
Department adscription.	Industrial Engineering
Research center/s	“Technological Research Center” and “Centre for Information and Communications Technology Research”
Code / Members Qty	G00087 / 21 members

Contact

Address	Avda. 19 de febrero s/n 15405 Ferrol, A Coruña, Spain
phone nº	+34 881013117
Fax	+34 981337401
email	jlcalvo@udc.es
web	http://investigacion.udc.es/es/Research/Details/G00087

Research scope

UNESCO Codes

- (120304) Artificial Intelligence
- (120305) Automated production systems
- (331105) Electrical control equipment
- (331107) Electronic Instruments
- (331101) Automation Technology
- (331102) Control engineering

Research lines

- Intelligent systems for modeling, optimization and control
- Fault and anomaly detection using traditional and intelligent techniques
- Knowledge creation for control, diagnosis and fault-tolerant systems
- New sensors, robust sensors and virtual sensors
- Artificial intelligence, neural networks and unsupervised learning

Technological offer

Services

- Data processing and analysis
- Modeling and simulation
- Programming of virtual instruments
- Automation and process optimization
- Development of virtual and electronic instrumentation
- Design and development of electronic power converters and circuits

Resources

- Mechanical vibration analysis system
- Embedded systems development platforms
- Platforms, and means of development, of automated systems
- Development of control, supervision and diagnosis systems
- Pilot plants for development and prototyping
- Robotic and computer vision systems
- Machining and additive manufacturing

Examples of research and transfer lines

Combined Cycle Power Plant

Endesa - As Pontes

Examples of research and transfer lines

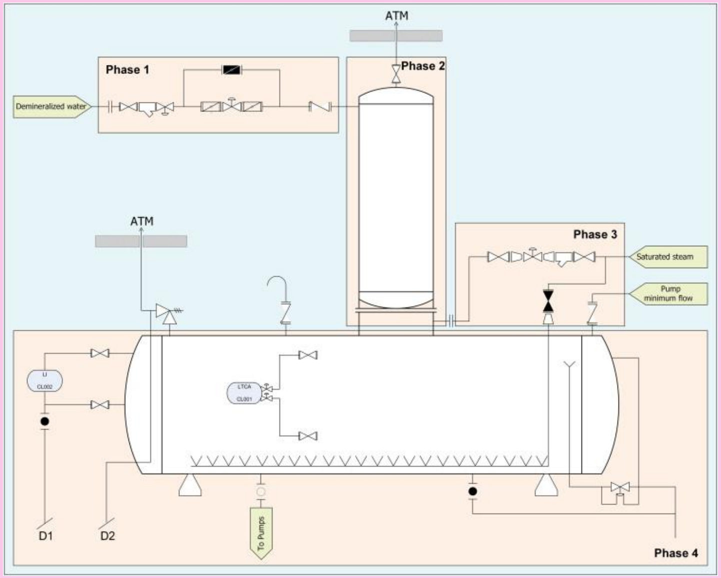

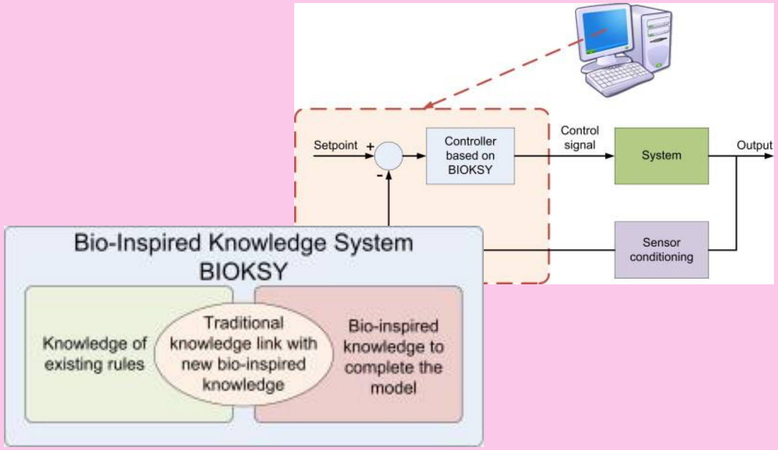

Steam turbine sealing circuit

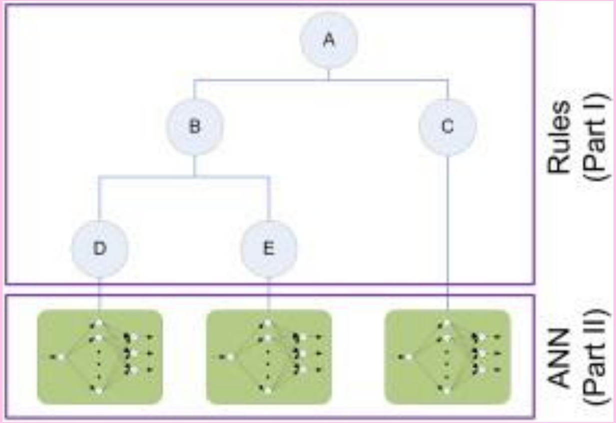

Examples of research and transfer lines

Metallurgy

Rolling process

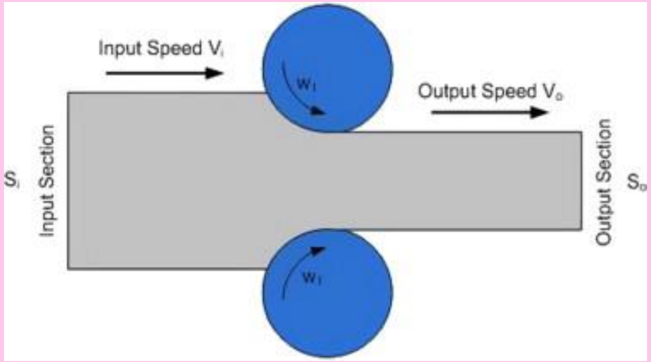

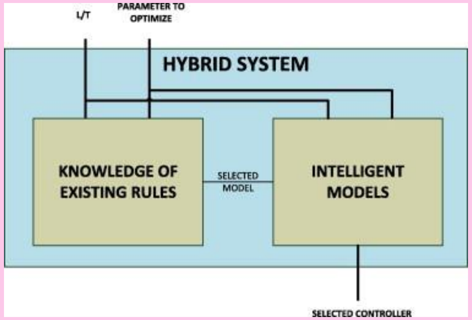

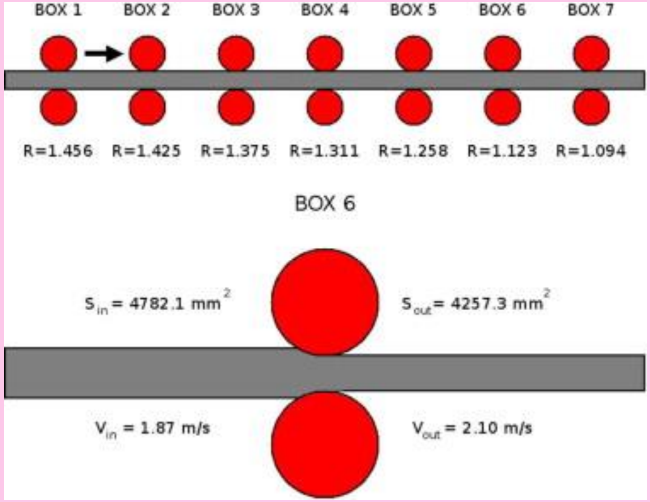

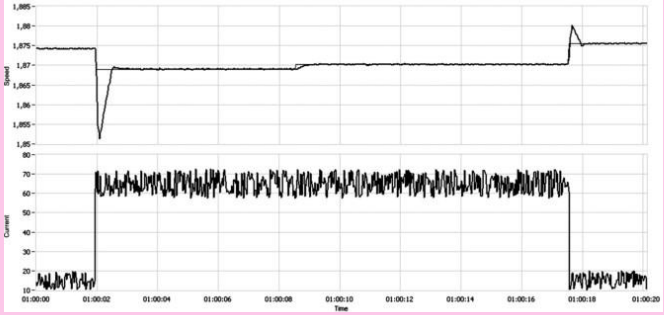

Examples of research and transfer lines

Bioclimatic house

Sotavento Galicia

Examples of research and transfer lines

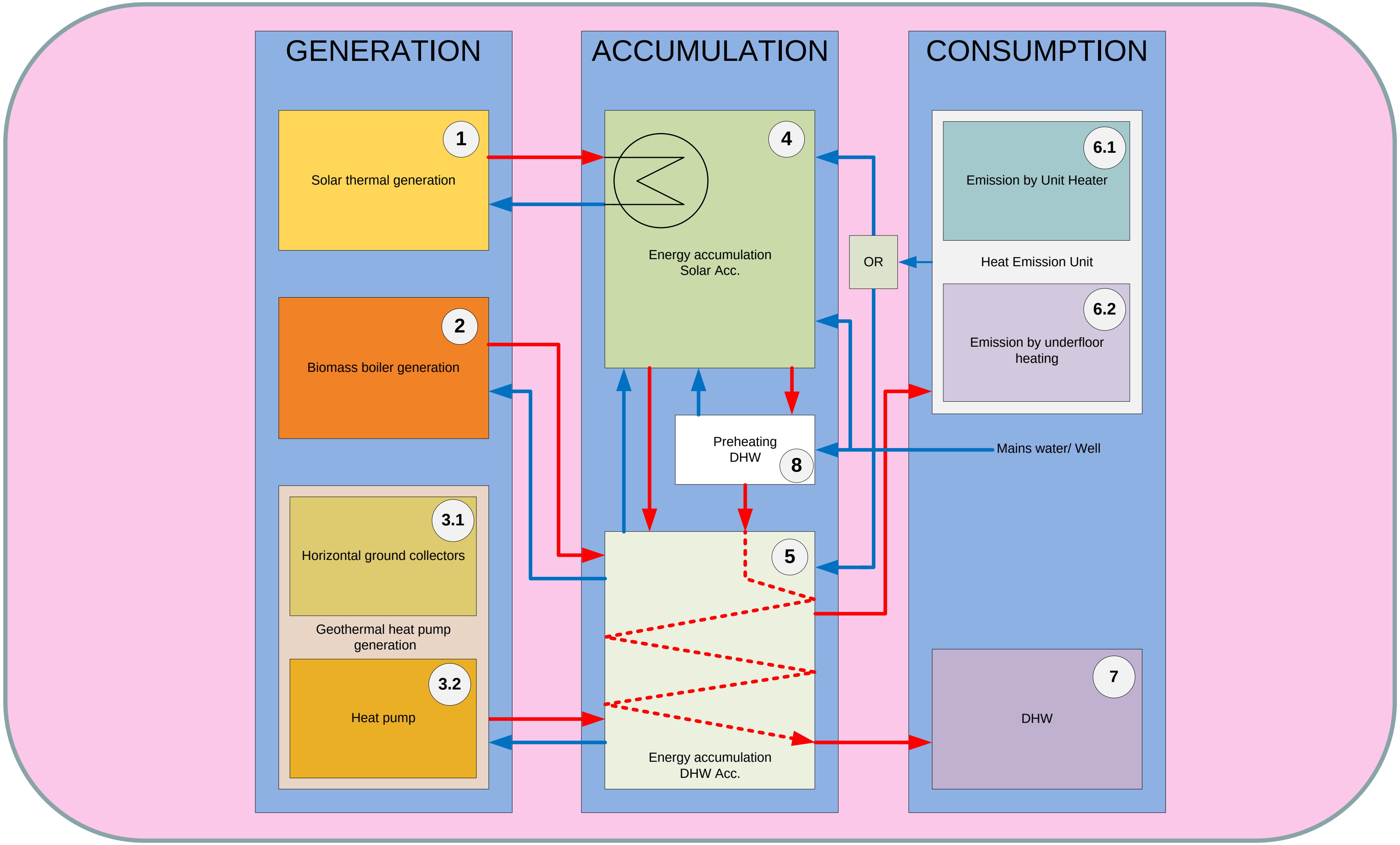

Examples of research and transfer lines

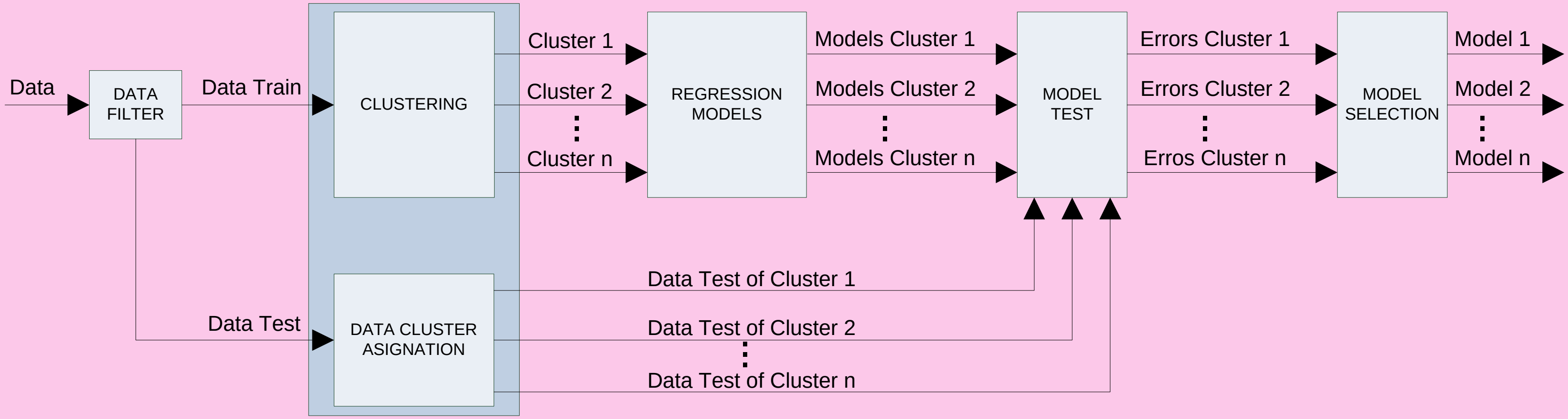

Solar thermal installation modeling

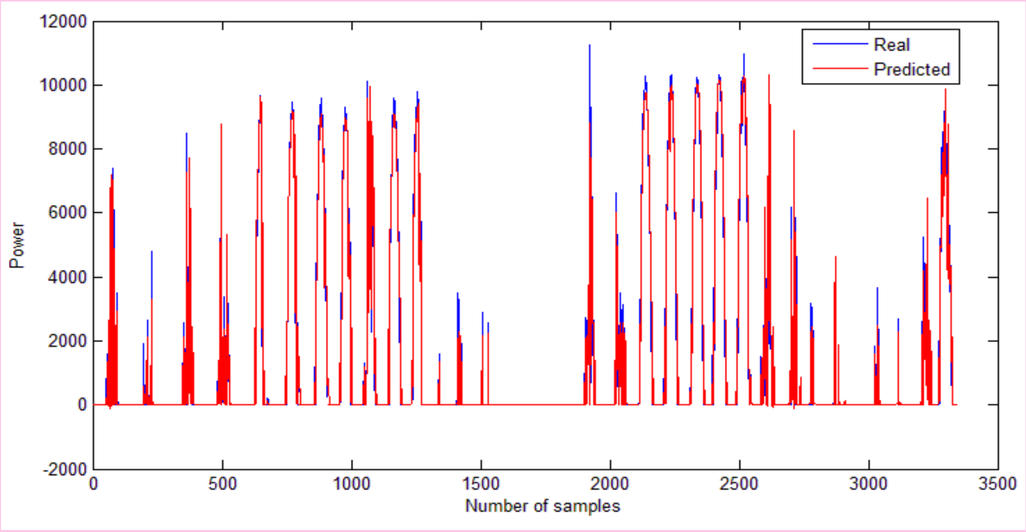

Examples of research and transfer lines

Cluster nº	Train samples	Test samples	MSE		
			ANN-MLP	Polynomial	LS-SVR
Cluster 1	9714	4874	0.00632	0.00882	0.00678
Cluster 2	6507	3257	0.00493	0.00926	0.00513
Cluster 3	12,433	6229	0.00613	0.01034	0.00671
Cluster 4	6479	3206	0.00598	0.00974	0.00632

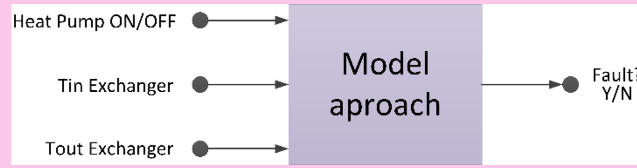

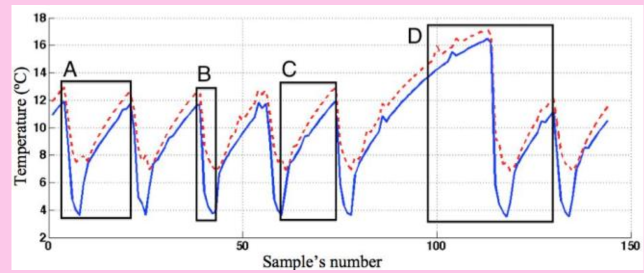

Geothermal heat exchanger installation:
- Modeling
- Fault detection

Examples of research and transfer lines

Anesthetic Control

ULL-UDC-HUC

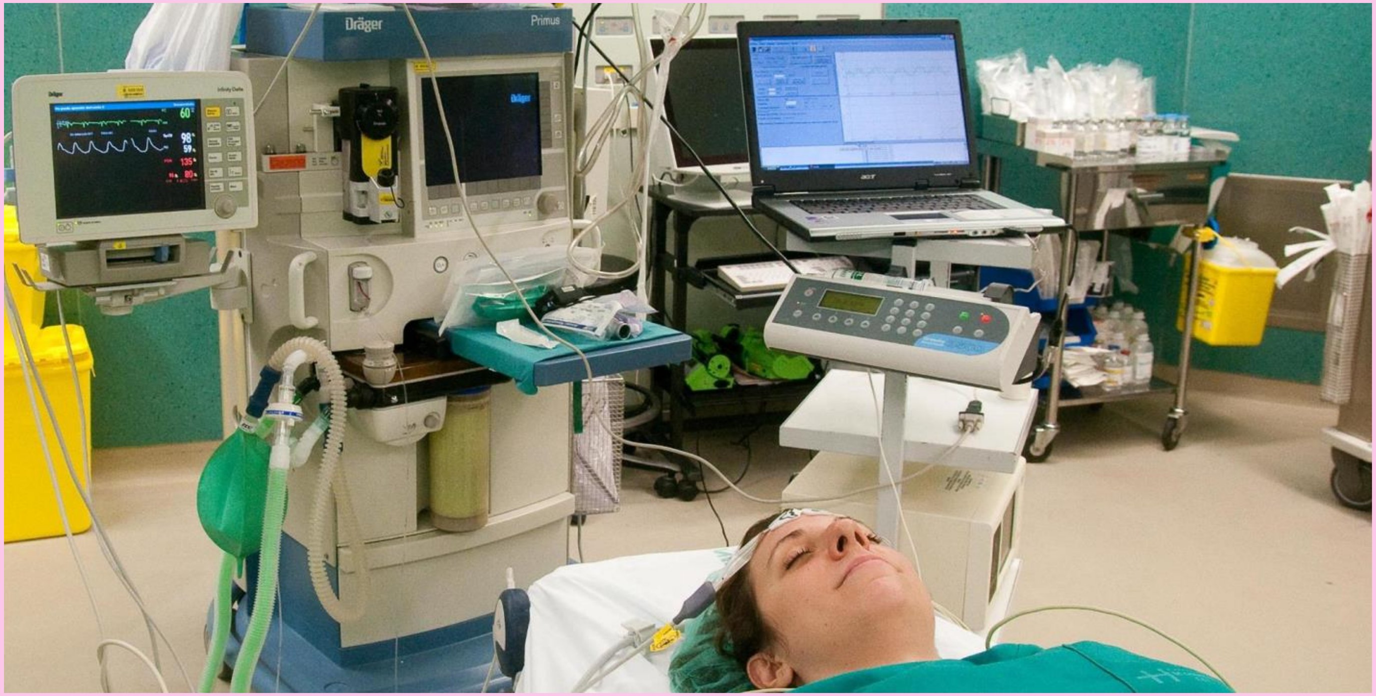

Examples of research and transfer lines

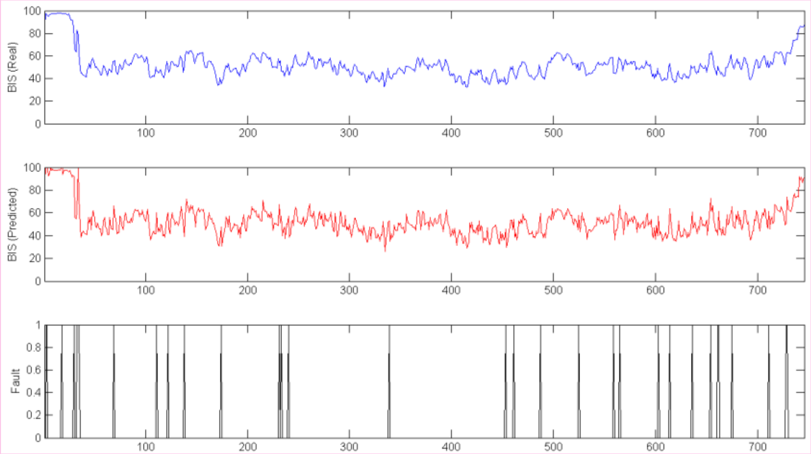

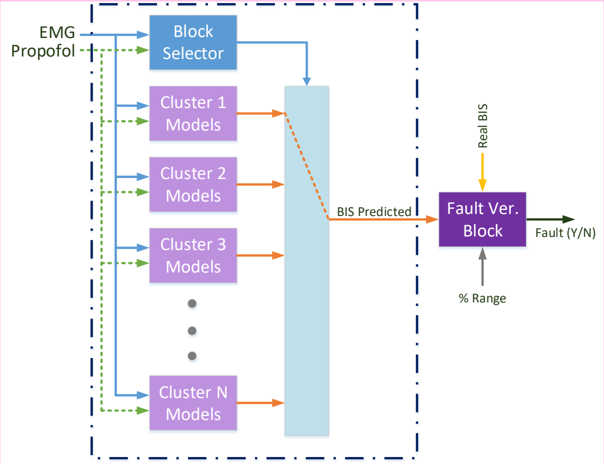

BIS and EMG:

- Modeling

- Anomaly detection

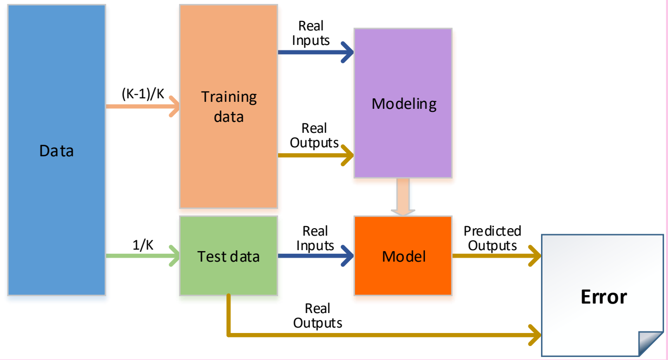

Examples of research and transfer lines

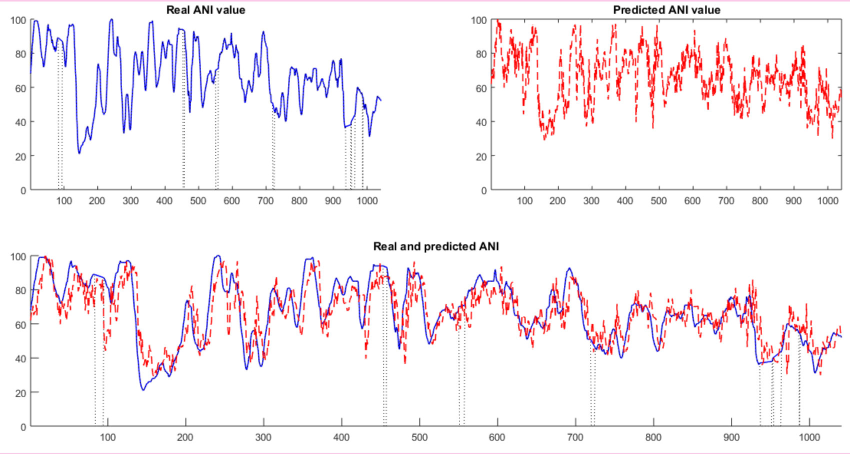

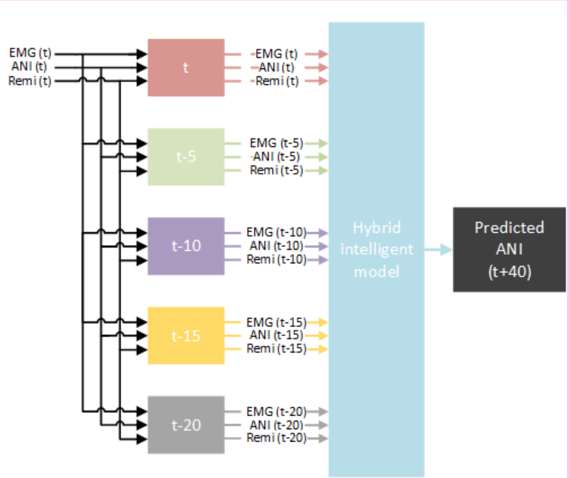

ANI:

- Modeling

- Anomaly detection

Brugada Syndrome

UDC - Uniovi - HCA

Intelligent classifiers:

- *Time domain parameters*
- *Frequency parameters*
- *Time series*

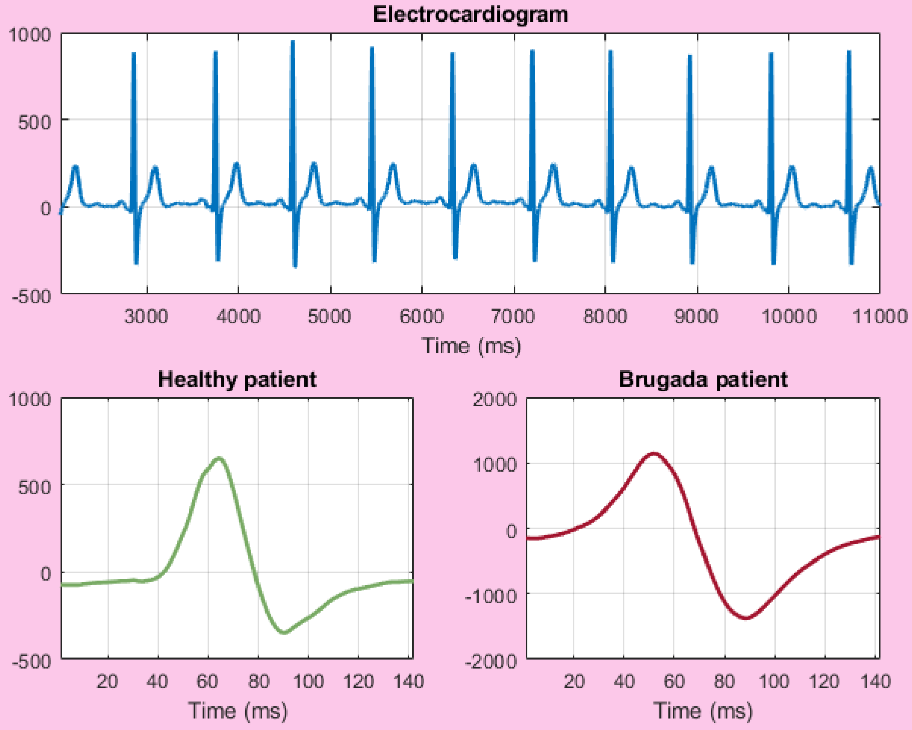

Examples of research and transfer lines

Anomaly detection (Traditional and emergent techniques)

Epoxy mixture – Control systems

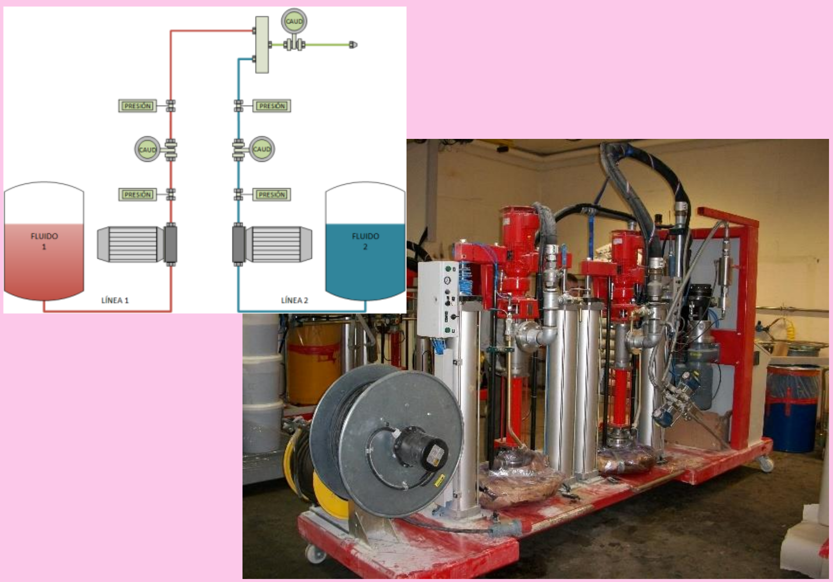

Fault detection, for predictive and conditional maintenance

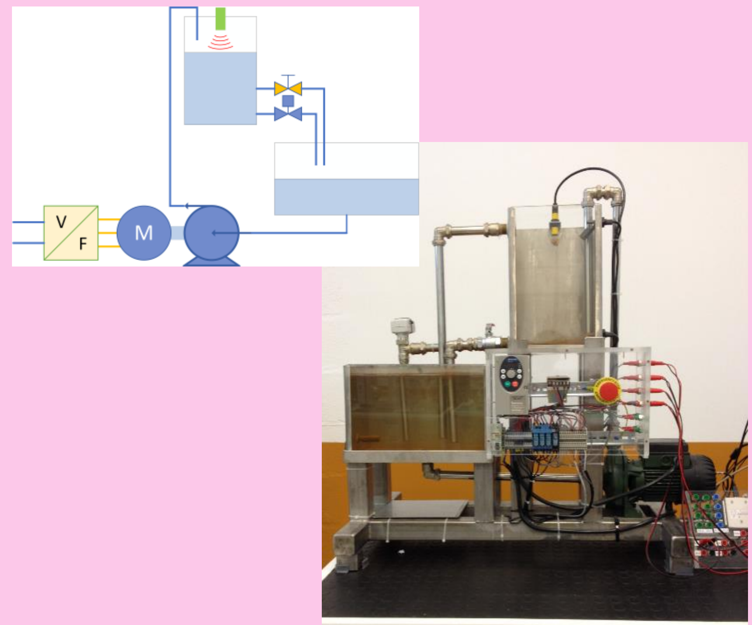

Systems for development of fault and anomaly detection algorithms

Examples of research and transfer lines

Development of electronic and virtual instrumentation and electronic converters

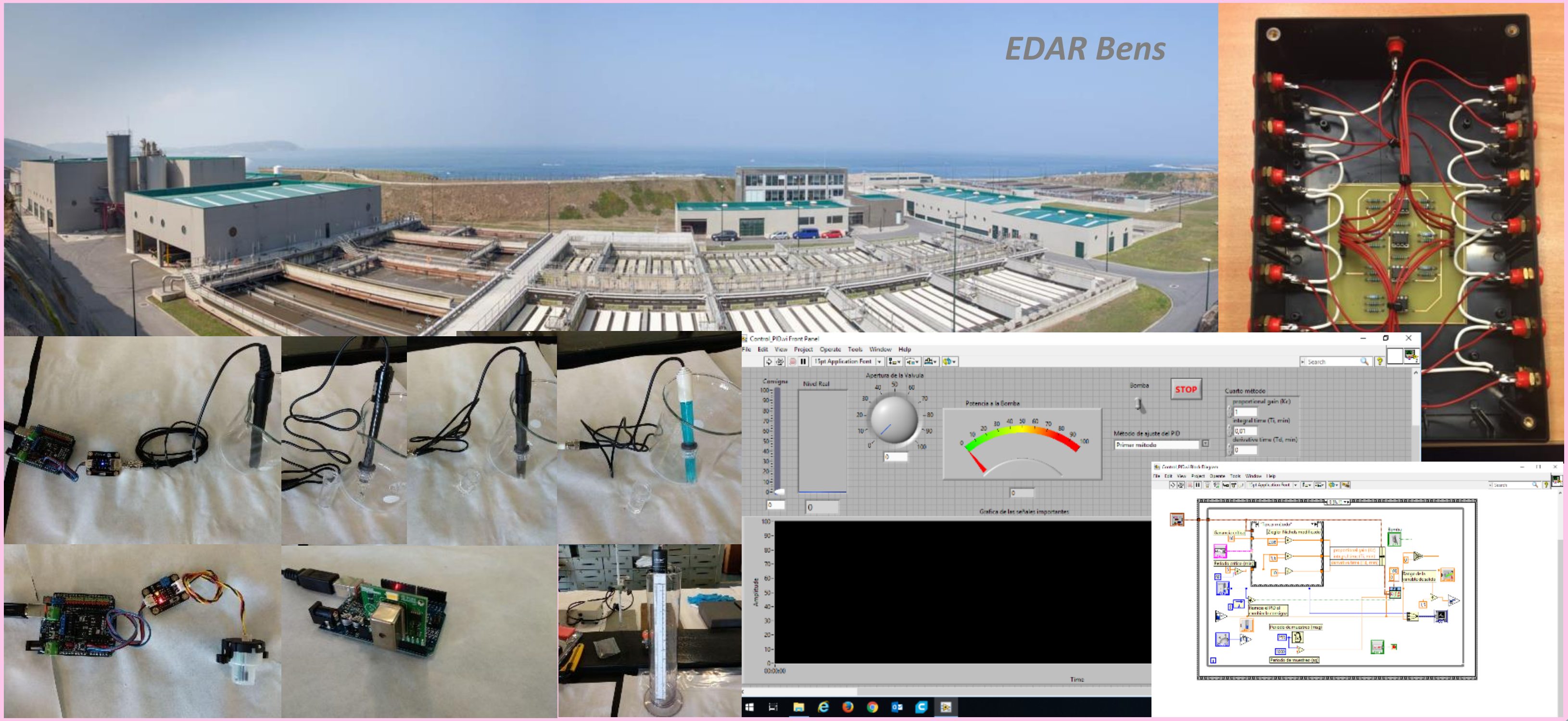

Examples of research and transfer lines

New Sensors - Biosensors

UDC

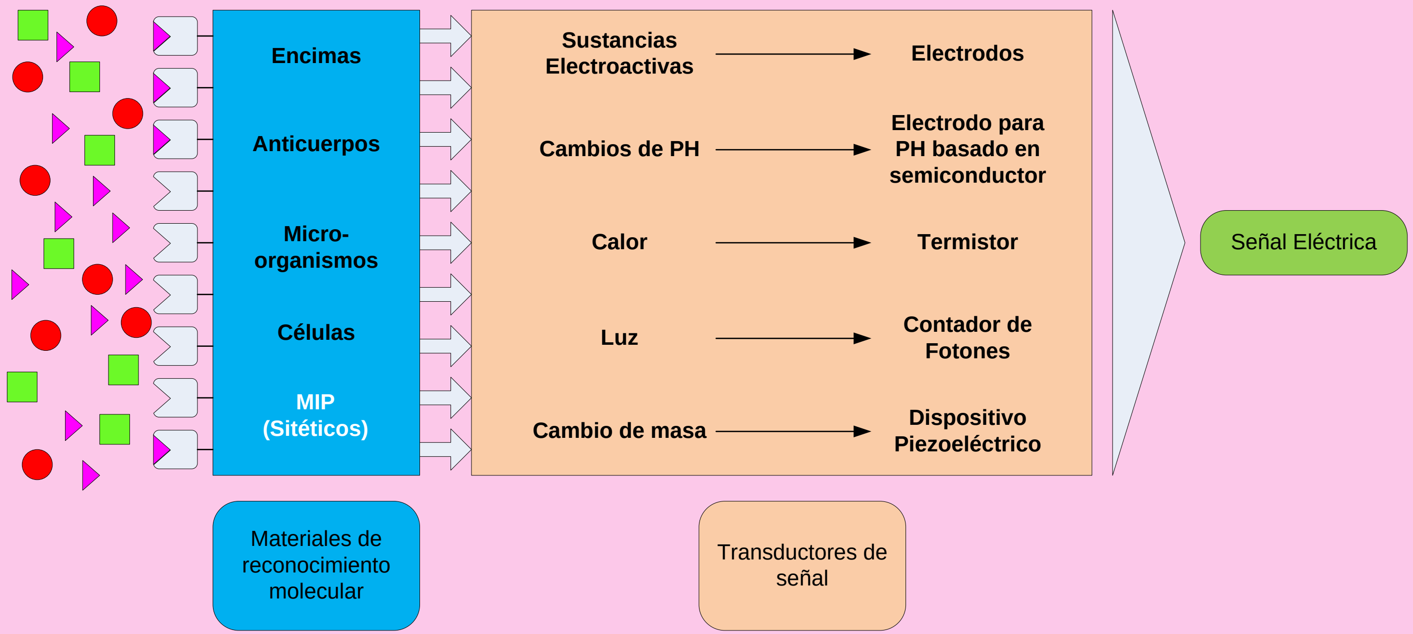

Examples of research and transfer lines

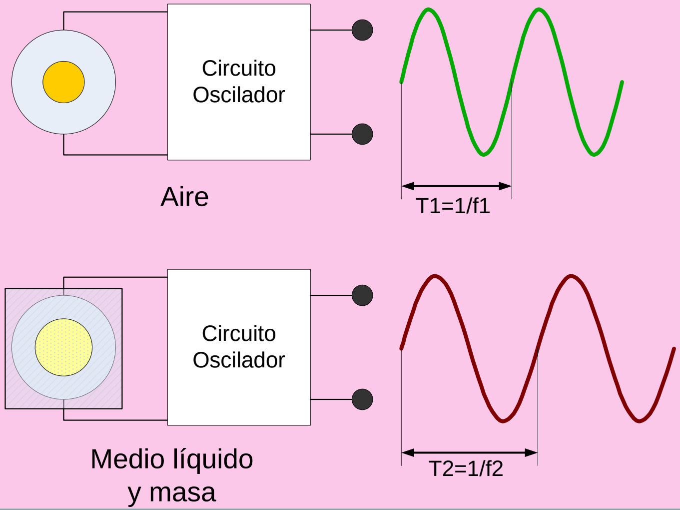

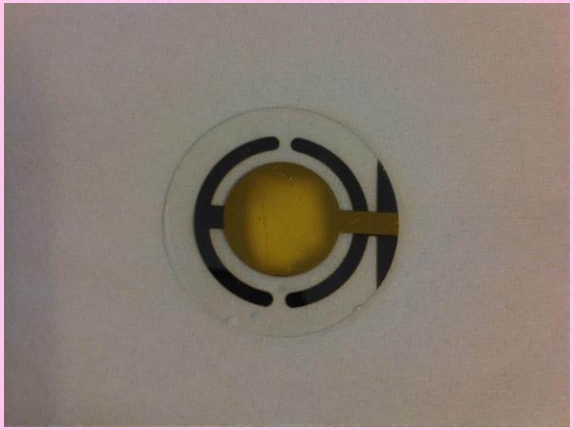

QCM-MIP:
- Characterization
- Biosensor

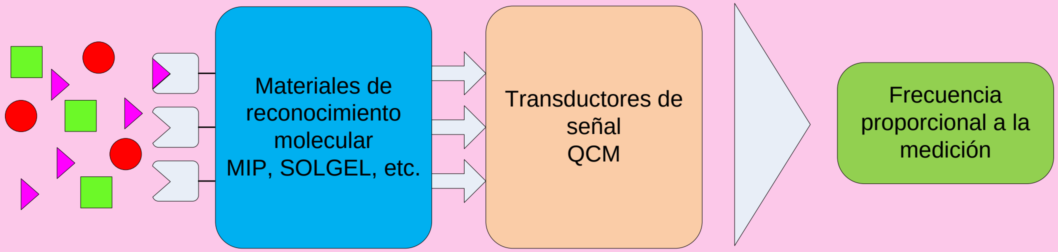

Examples of research and transfer lines

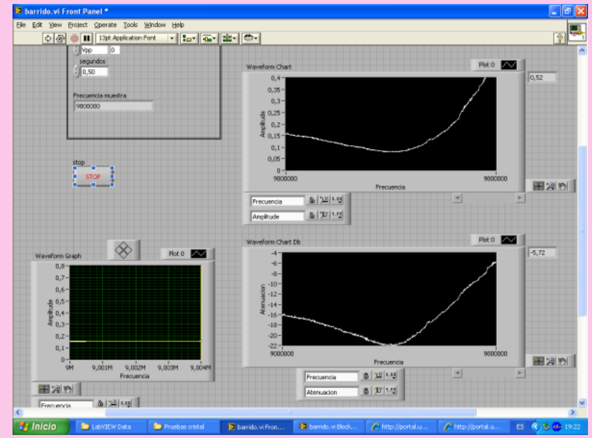

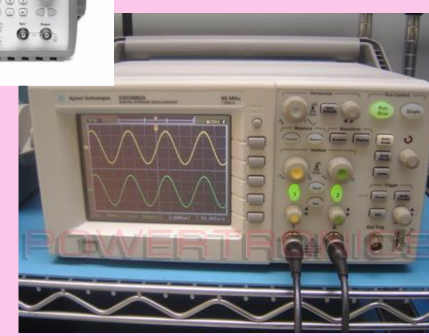

QCM-MIP:

- Characterization

- Biosensor

Examples of research and transfer lines

Laboratory plants development for research in teaching in control

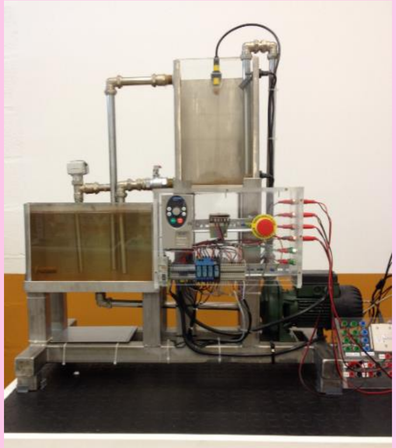

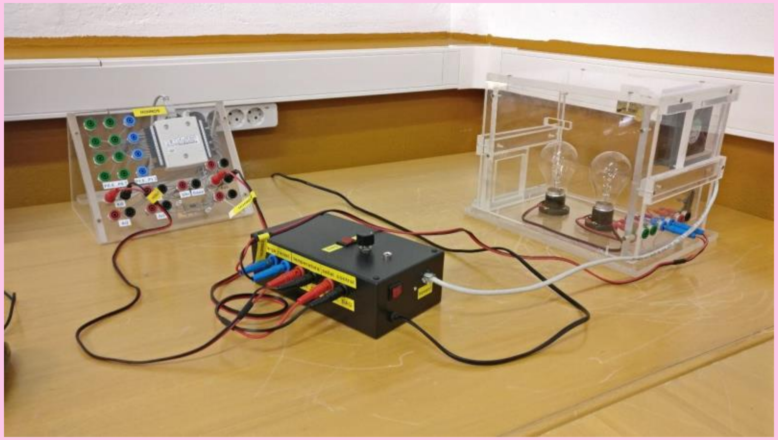

Examples of research and transfer lines

Intelligent Digital Industry / Industrial Computing and Automation - ("IDI/IIA")

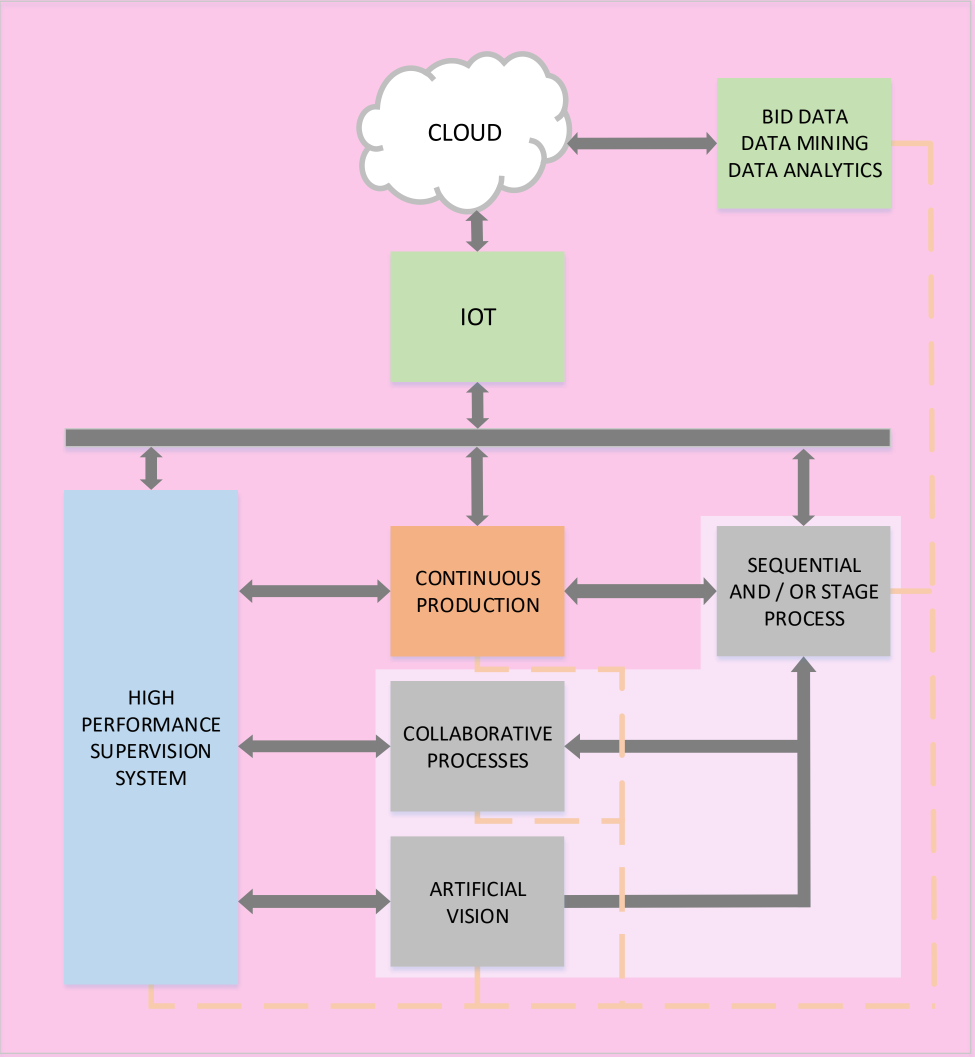

Examples of research and transfer lines

Basic research for Optimization, Modeling and Control

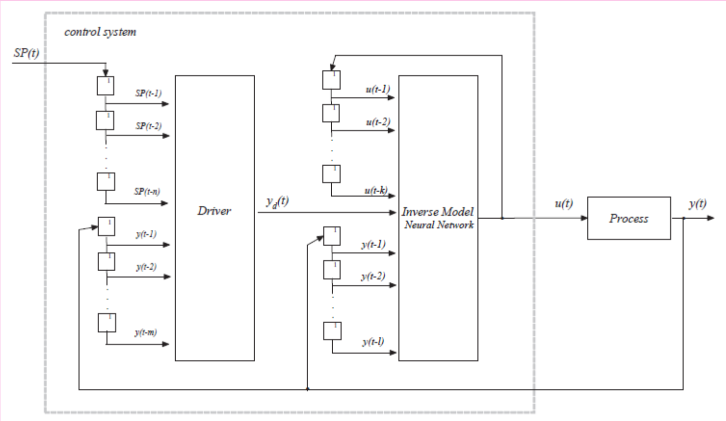

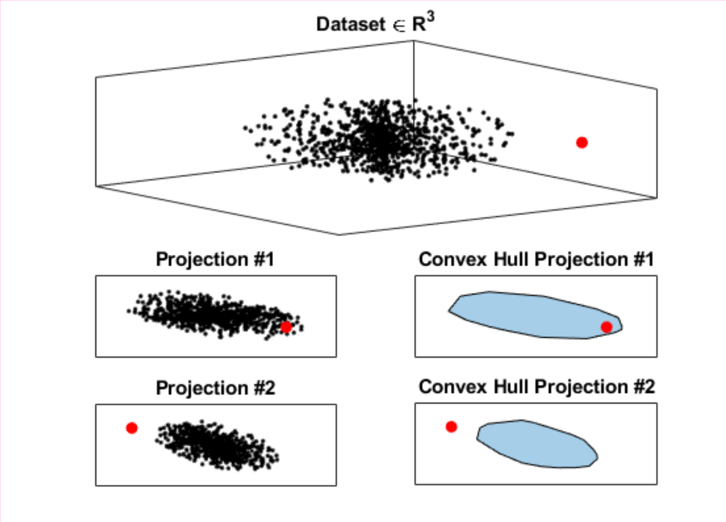

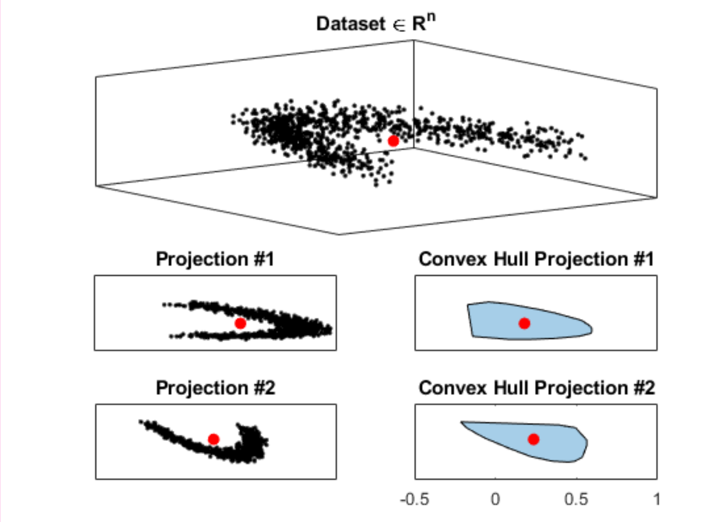

A HYBRID REGRESSION SYSTEM BASED ON LOCAL MODELS FOR SOLAR ENERGY PREDICTION

A Hybrid Regression System Based on Local Models for Solar Energy Prediction

- Case of Study

A Hybrid Regression System Based on Local Models for Solar Energy Prediction

- Case of Study

A Hybrid Regression System Based on Local Models for Solar Energy Prediction

- Case of Study

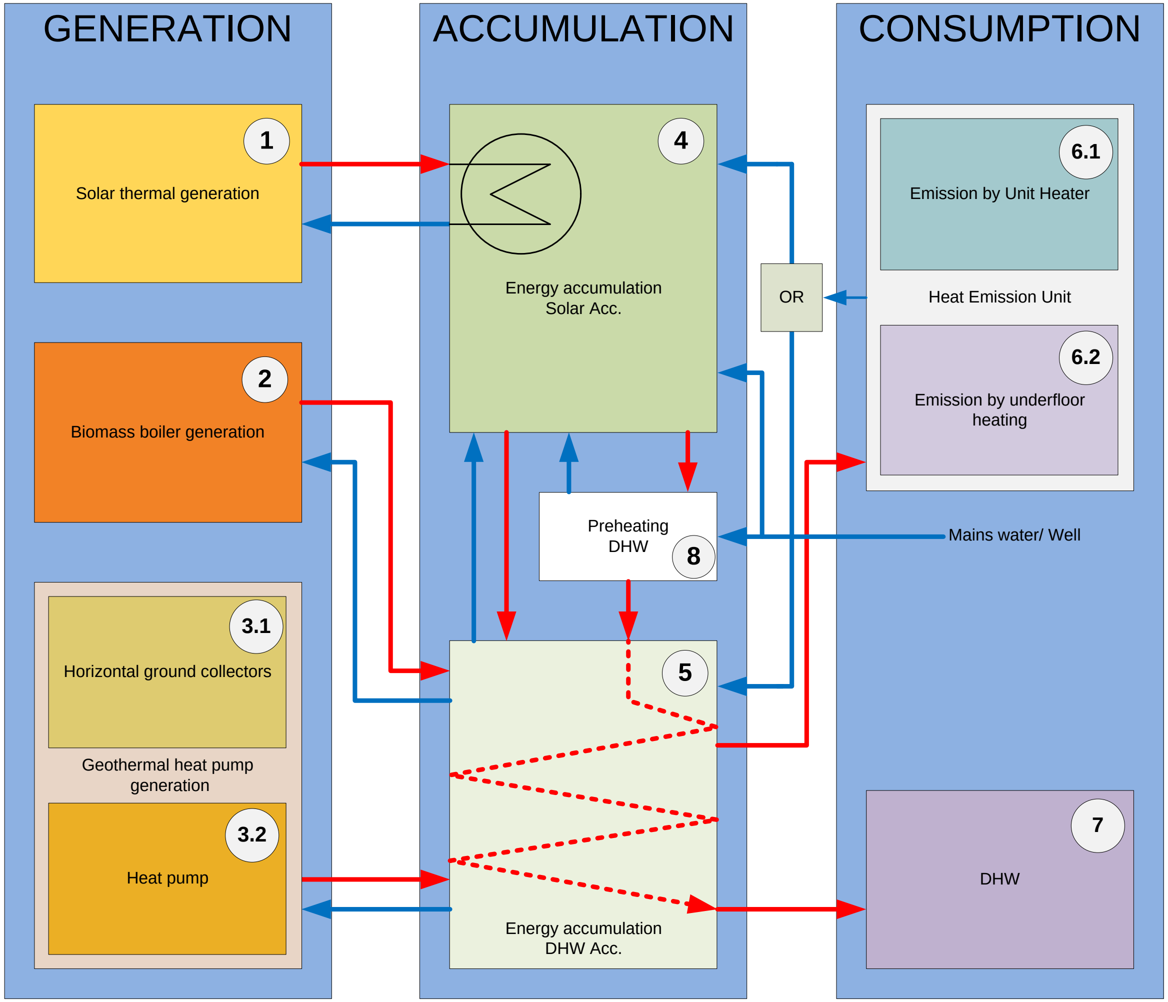

A Hybrid Regression System Based on Local Models for Solar Energy Prediction

- Case of Study

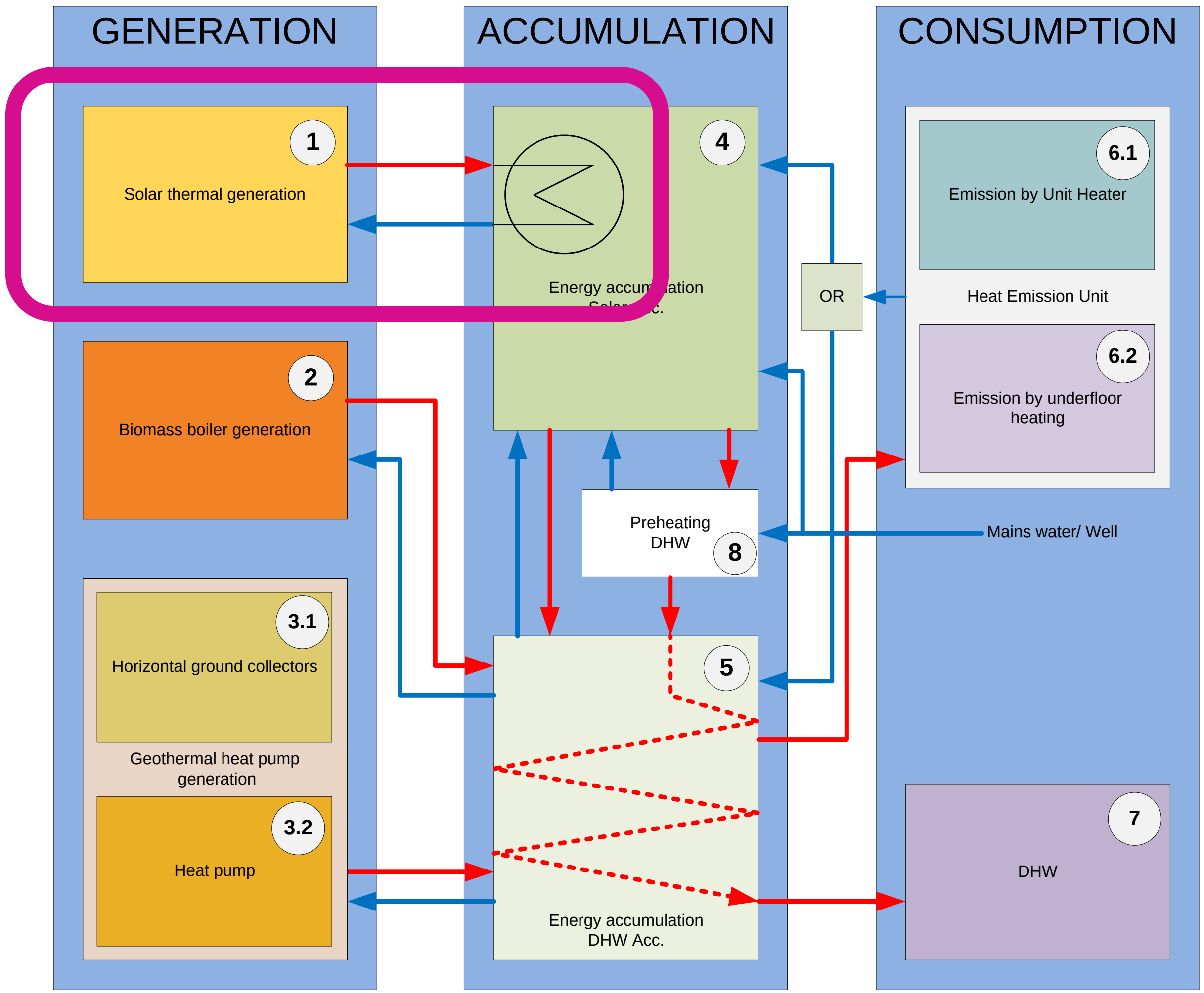

- Case of Study

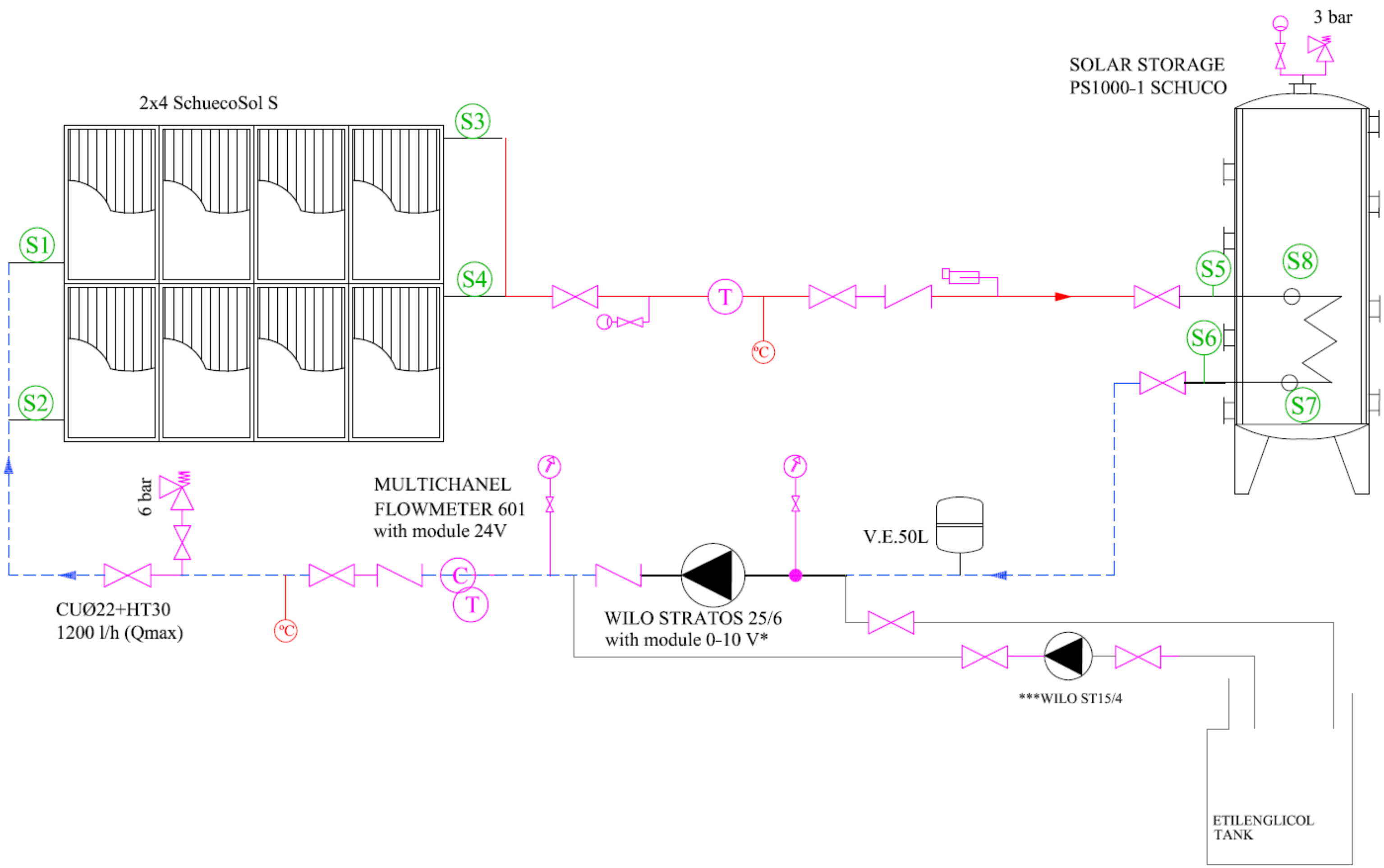

- Data description summarized:
  - Data set of 36,292 samples (12 months)
  - Two inputs:
    - Flow in the solar thermal circuit
    - Solar radiation
  - One output:
    - Thermal power generated by the solar thermal system
- Equipment
  - Power meter: Kamstrup type Multichannel 601, it can measure thermal power, flow and temperature.
  - Radiation meter: Apogee model PYR-P, it can measure solar radiation with a sensitivity of 0.200 mV per W/m2.

A Hybrid Regression System Based on Local Models for Solar Energy Prediction

- Modeling approach and comparison:

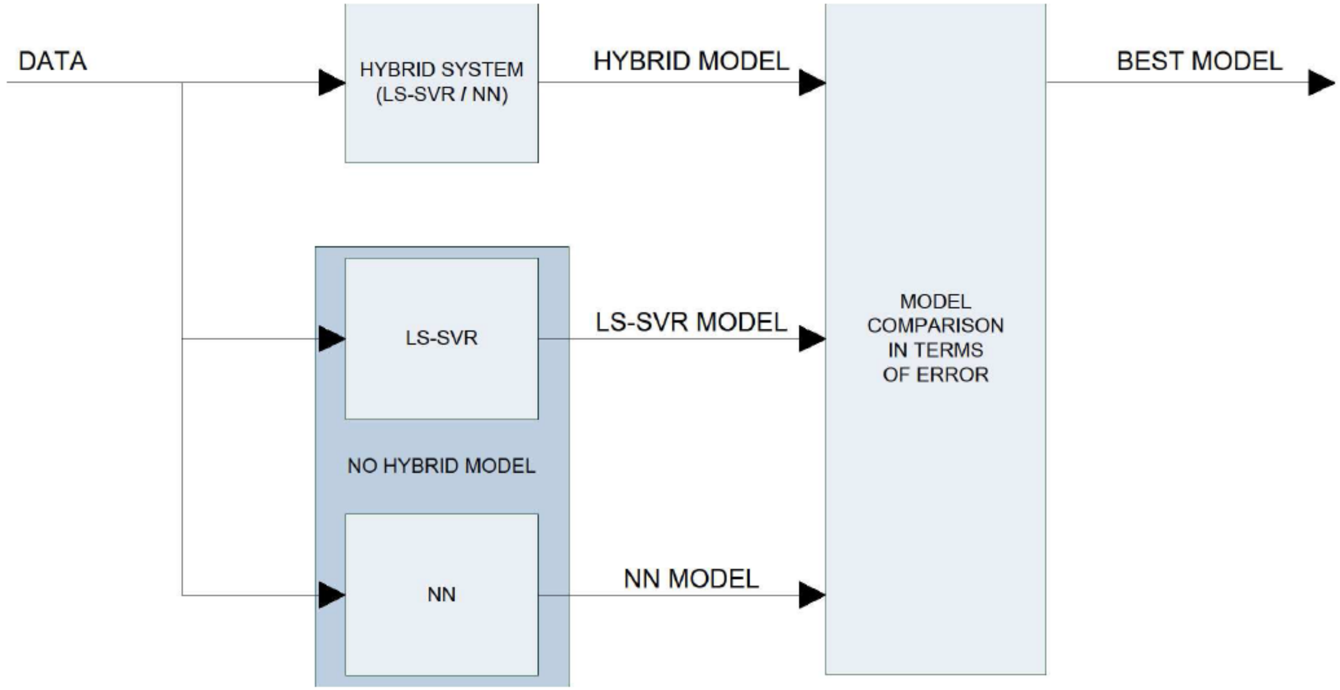

A Hybrid Regression System Based on Local Models for Solar Energy Prediction

- Modeling approach and comparison:

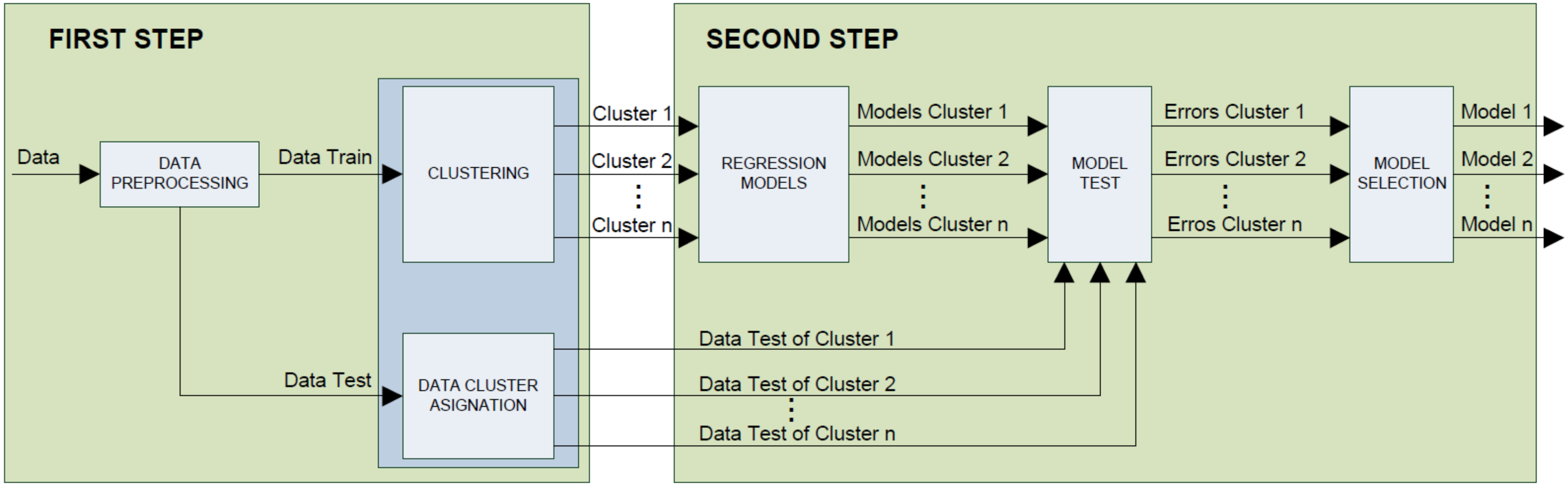

A Hybrid Regression System Based on Local Models for Solar Energy Prediction

- Methods
  - Clustering:
    - Principal Components Analysis (PCA)
    - Self-organizing map (SOM)
  - Regression:
    - Artificial Neural Network (ANN)
    - Least Square Support Vector Machine (SVM: LS-SVM)
  - Cross validation of 10 folds for all regression techniques.

A Hybrid Regression System Based on Local Models for Solar Energy Prediction

- Clustering Results

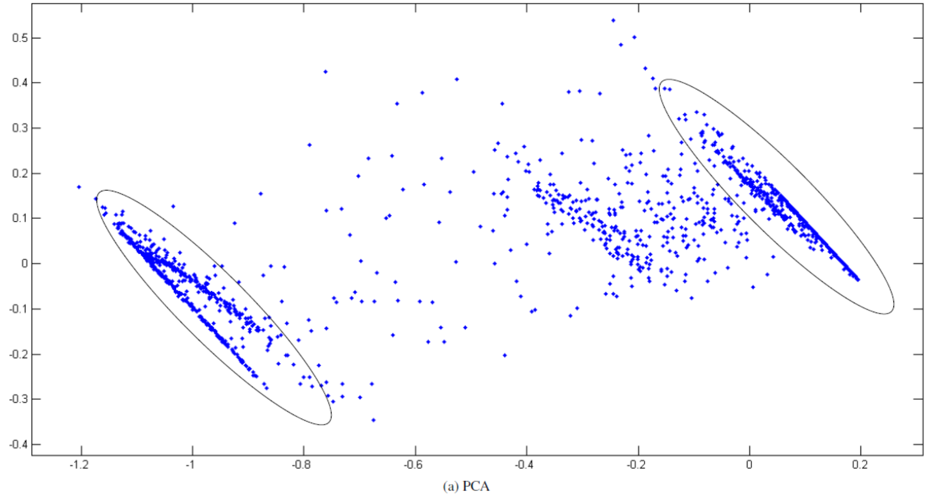

(a) PCA

- SOM technique can detect three different clusters.
- The sample cluster assignment is made by the euclidean distance.

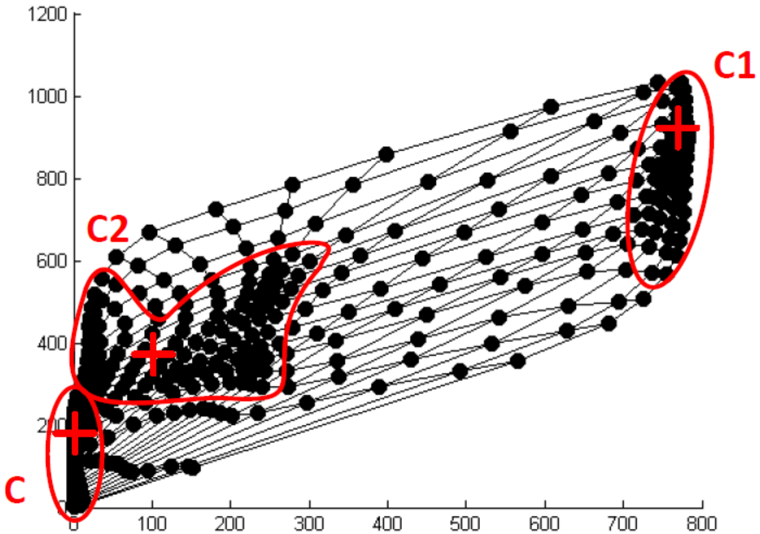

(b) SOM

A Hybrid Regression System Based on Local Models for Solar Energy Prediction

- Clustering Results

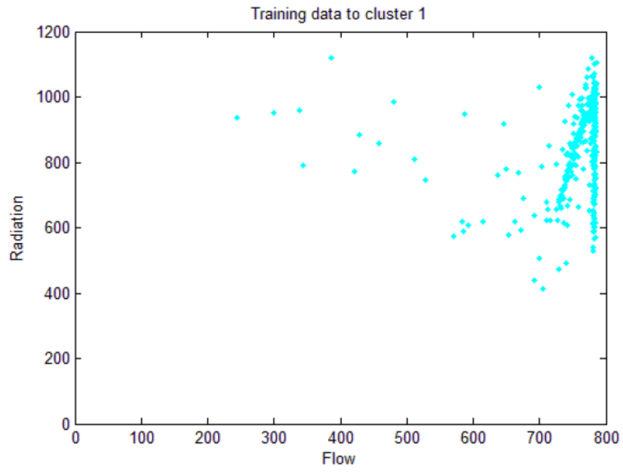

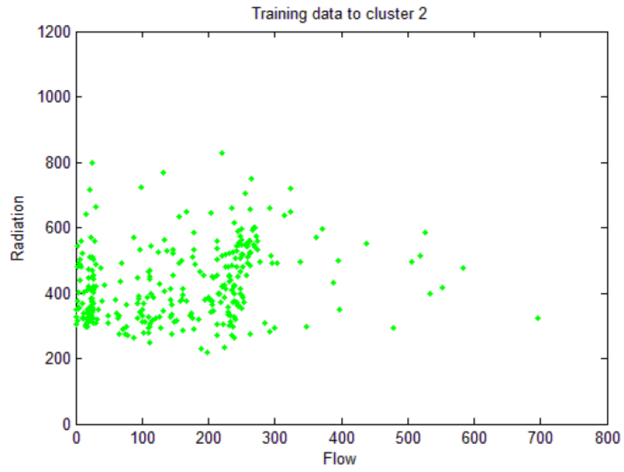

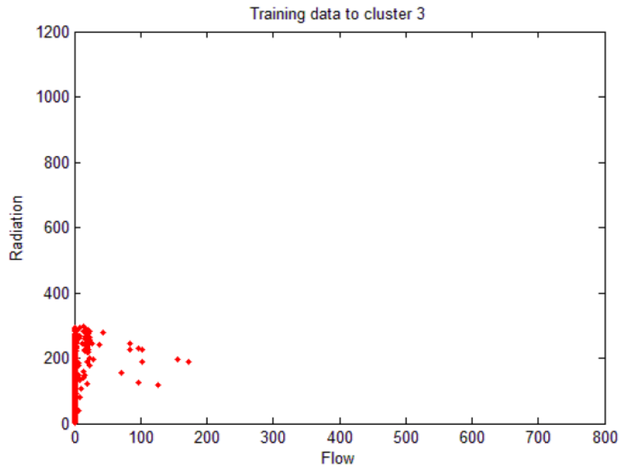

- Clustering Results

Total number of samples for training and testing for each month before and after clustering.

Month	Total		Cluster 1		Cluster 2		Cluster 3	
	Train	Test	Train	Test	Train	Test	Train	Test
January (2011)	2221	1111	1571	776	250	144	400	191
February (2011)	2205	1102	1568	769	211	104	426	229
March (2011)	2230	1115	1458	733	236	130	536	252
April (2011)	1819	909	948	453	206	126	665	330
May (2011)	2012	1006	1107	560	268	131	637	315
June (2011)	2040	1021	1189	600	260	136	591	285
July (2011)	2000	1000	1229	613	245	116	526	271
August (2011)	2001	1000	1211	604	237	133	553	263
September (2010)	2880	1440	1940	971	281	144	659	325
October (2010)	1400	700	817	412	185	73	398	215
November (2010)	1384	693	905	459	189	96	290	138
December (2010)	2002	1001	1414	722	232	93	356	186

A Hybrid Regression System Based on Local Models for Solar Energy Prediction

- Regression results

Values of NMSE of the hybrid system.

Month	Hybrid								
	LS-SVR				ANN				Combined
	C1	C2	C3	Total	C1	C2	C3	Total	Total
January	0.0146	0.4211	0.0870	0.0494	0.0102	0.5184	0.0648	**0.0369**	**0.0358**
February	0.3973	0.3501	0.0796	**0.0316**	0.6518	0.3810	0.0813	0.0323	0.0316
March	0.3090	0.1961	0.0733	0.0230	0.2716	0.2160	0.0612	**0.0199**	**0.0191**
April	0.6294	0.0540	0.0120	**0.0113**	0.8663	0.1649	0.0235	0.0246	0.0113
May	0.2962	0.3278	0.2352	**0.0601**	0.4166	0.4083	0.2370	0.0621	0.0601
June	0.1770	0.3144	0.1954	**0.0508**	0.7445	0.3387	0.1924	0.0517	**0.0501**
July	0.3196	0.3810	0.1937	**0.0466**	0.4013	0.4185	0.2199	0.0527	0.0466
August	0.1739	0.3907	0.1741	**0.0393**	0.7408	0.3667	0.1977	0.0441	**0.0390**
September	0.7069	0.2751	0.0948	**0.0364**	0.8510	0.2620	0.0981	0.0376	**0.0363**
October	0.8036	0.1799	0.1391	**0.0319**	0.8341	0.2300	0.1443	0.0359	0.0319
November	0.2013	0.3809	0.1441	**0.0355**	0.8608	0.4082	0.1364	0.0447	**0.0322**
December	0.5034	0.6418	0.1654	**0.0510**	0.1649	0.6032	0.2017	0.0627	**0.0489**

NMSE of non-hybrid system.

Non-hybrid												
Month	Jan.	Feb.	Mar.	Apr.	May	Jun.	Jul.	Aug.	Sep.	Oct.	Nov.	Dec.
LS-SVR	0.129	0.159	0.116	0.115	0.194	0.211	0.187	0.183	0.156	0.105	0.120	0.219
ANN	0.181	0.203	0.128	0.098	0.299	0.246	0.269	0.187	0.168	0.134	0.083	0.227

A Hybrid Regression System Based on Local Models for Solar Energy Prediction

- Graphical results

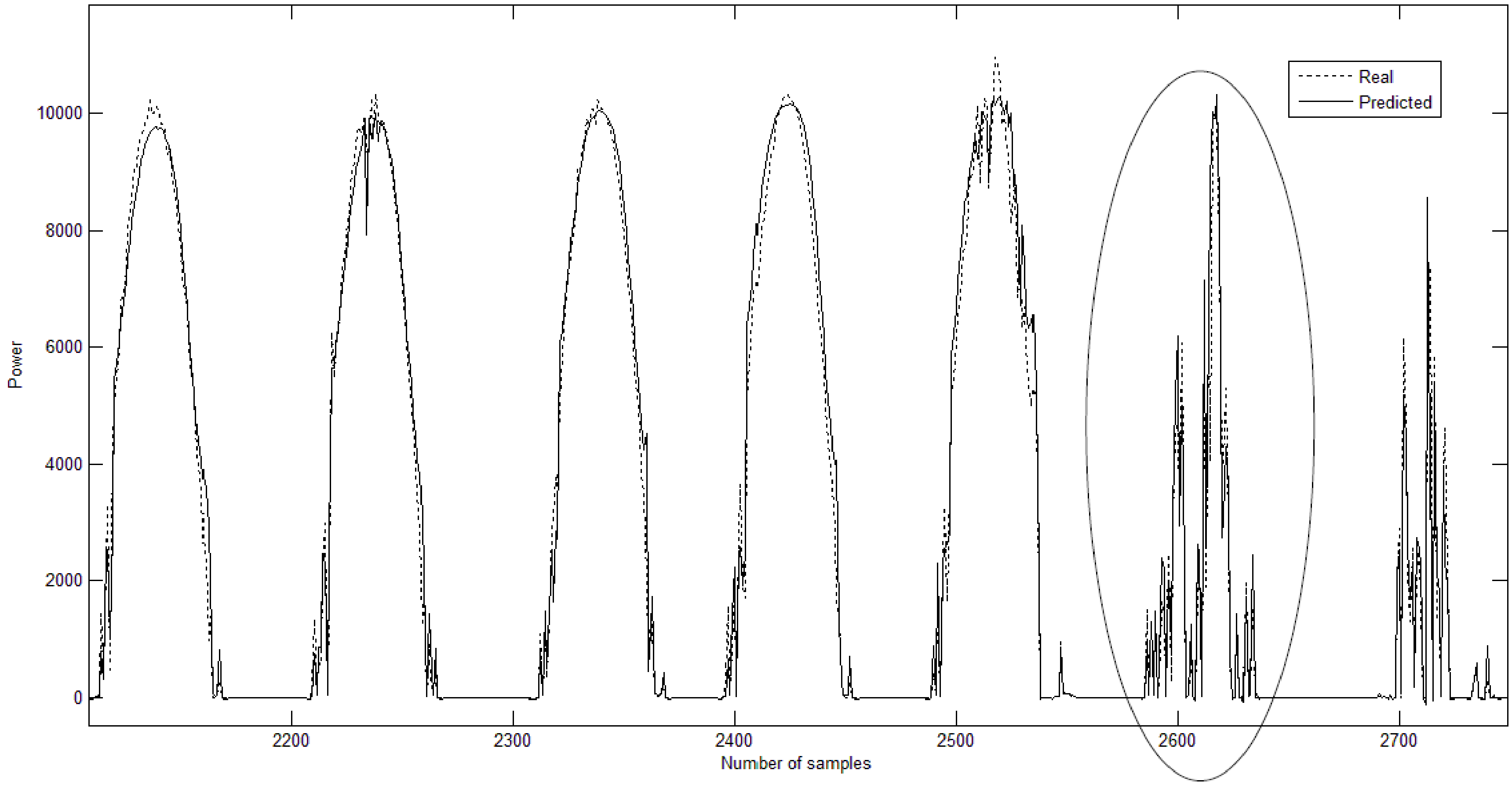

- Graphical results

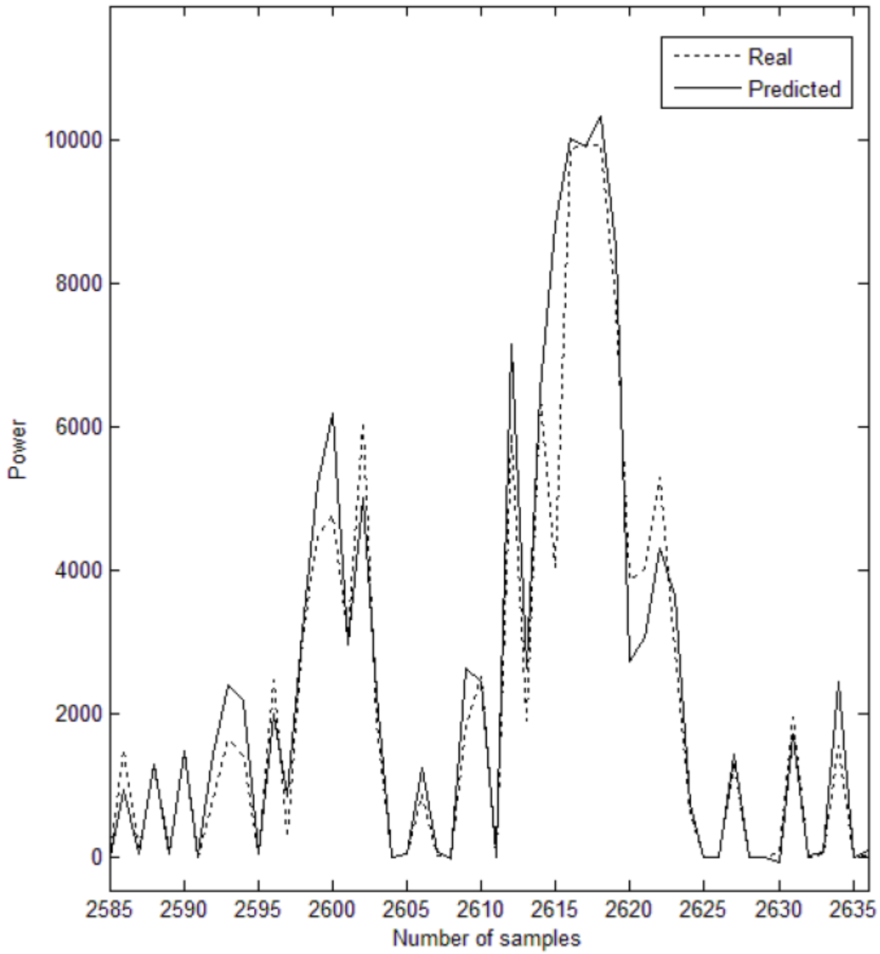

- Conclusions
  - It has been achieved a very nice accuracy.
  - The hybrid proposal gives better results than the non hybrid one.
  - The cluster creation process is not fully automatic, this fact can be good or bad.

HYBRID INTELLIGENT MODEL METHODOLOGY

Hybrid intelligent model Methodology

- The system - Operating points

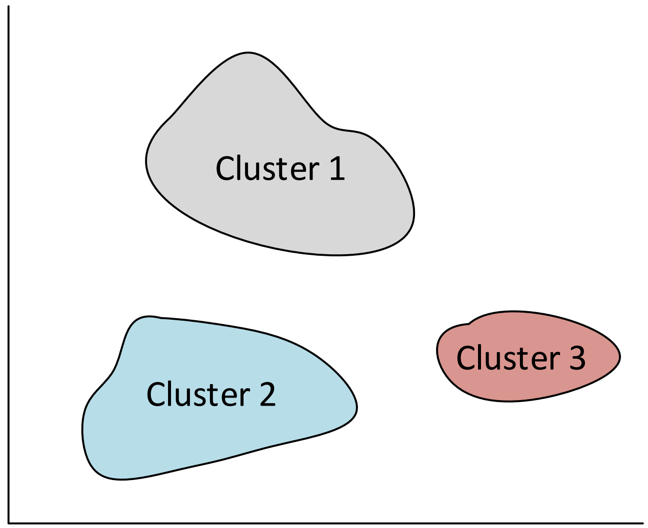

Hybrid intelligent model Methodology

- Modeling process

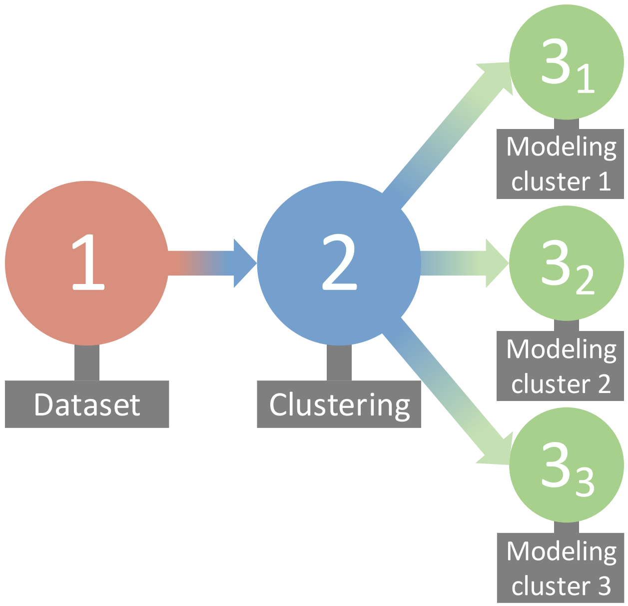

Hybrid intelligent model Methodology

- Modeling process.
  - Clustering (automatic, not like in the previous case).
    - Kmeans.

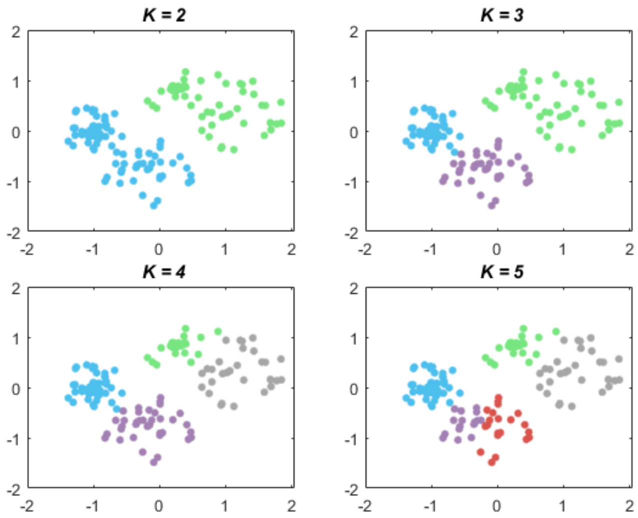

$$E(c_1, ..., c_K) = \sum_{i=1}^{N} \sum_{j=1}^{K} I(x_i \in G_j) \, ||x_i - c_j||$$

Hybrid intelligent model Methodology

- Modeling process.
  - Clustering.
  - Modeling.
    - MLP.

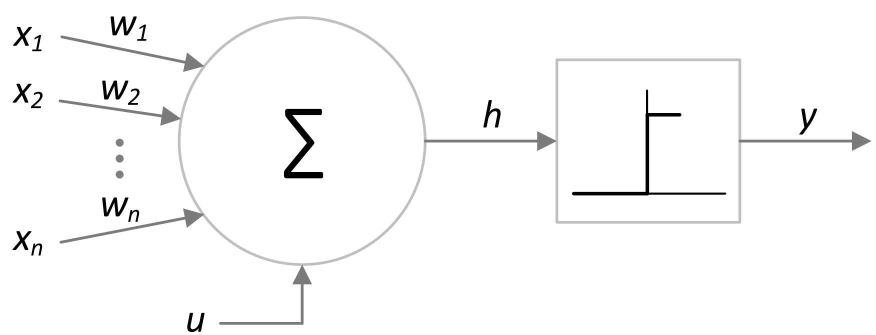

Hybrid intelligent model Methodology

- Modeling process.
  - Clustering.
  - Modeling.
    - MLP.

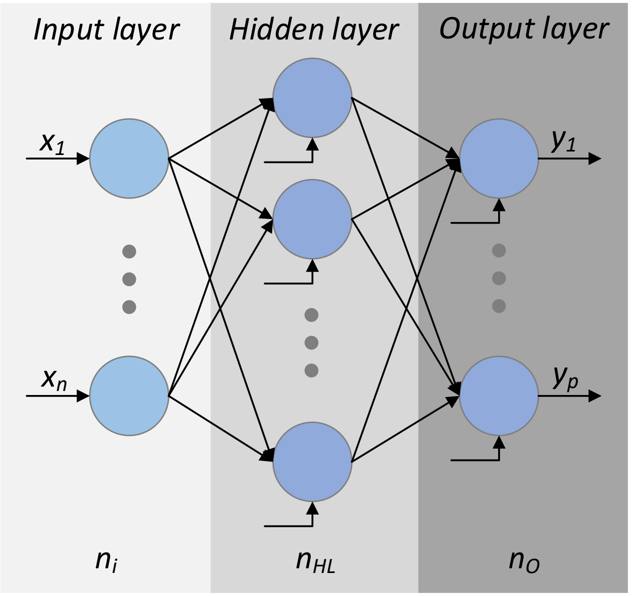

$$h = f_{\theta 1}\left(xW_1 - u_1\right)$$

$$y = f_{\theta 2}\left(hW_2 - u_2\right)$$

Hybrid intelligent model Methodology

- Modeling process.
  - Clustering.
  - Modeling.
    - MLP.
    - LS SVR

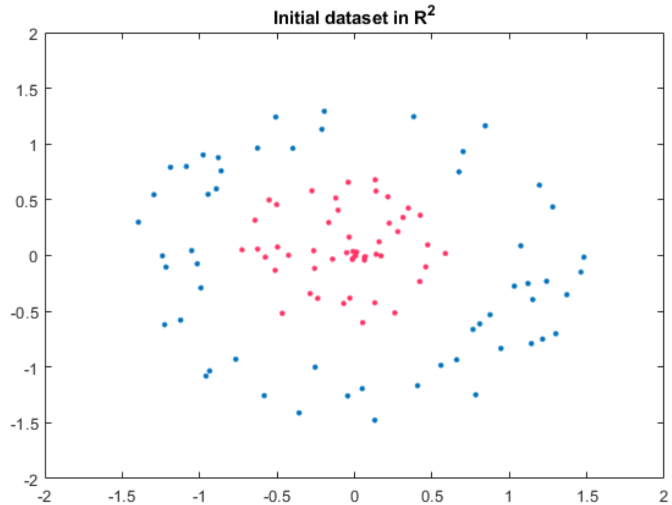

$$y = f(X) = w^T \delta(x) + b$$

Hybrid intelligent model Methodology

- Modeling process.
  - Clustering.
  - Modeling.
    - MLP.
    - LS SVR

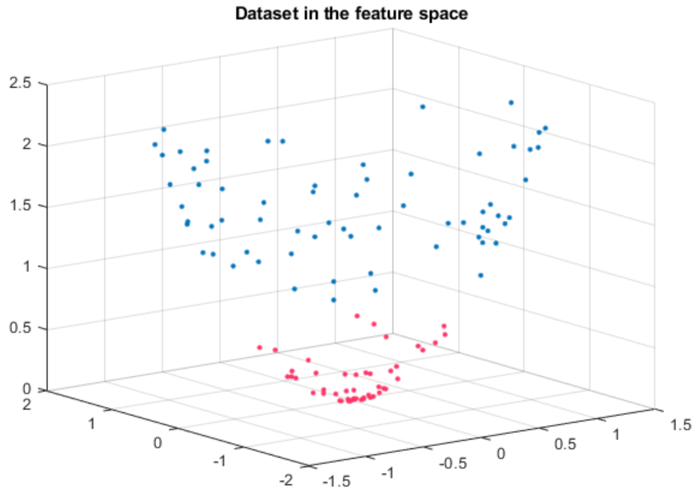

$$y = f(X) = w^T \delta(x) + b$$

Hybrid intelligent model Methodology

- Modeling process.
  - Clustering.
  - Modeling.
  - Validation.

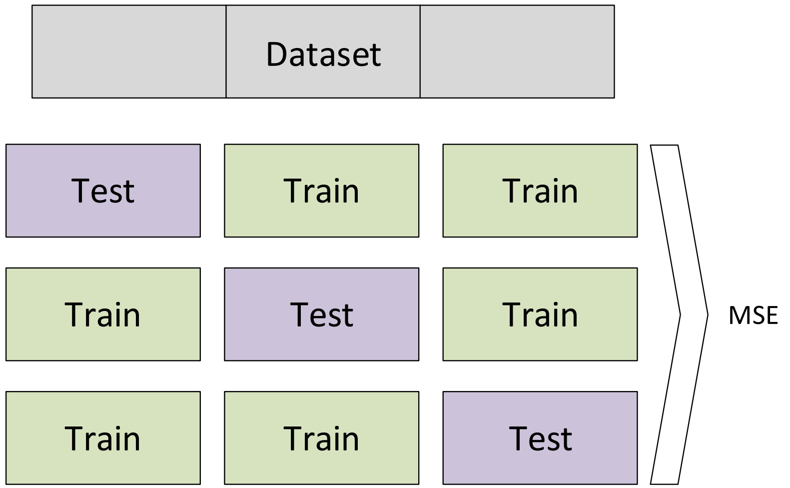

Hybrid intelligent model Methodology

- Modeling process.
  - Clustering.
  - Modeling.
  - Validation.
  - Best configuration.

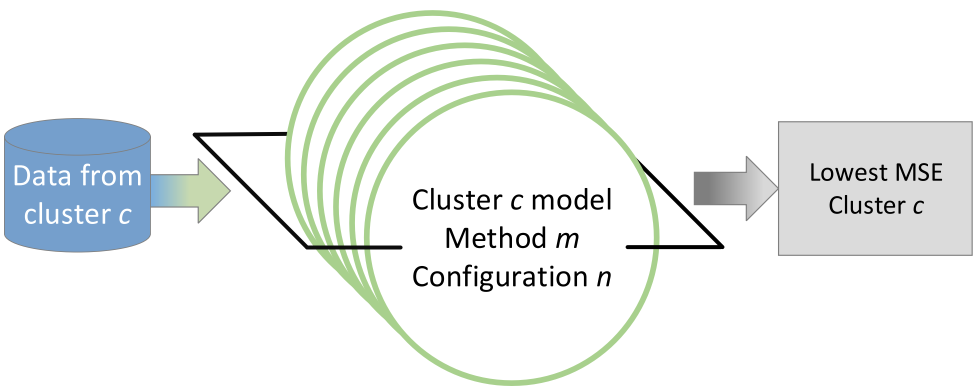

Hybrid intelligent model Methodology

- Modeling process.
  - Clustering.
  - Modeling.
  - Validation.
  - Best configuration.

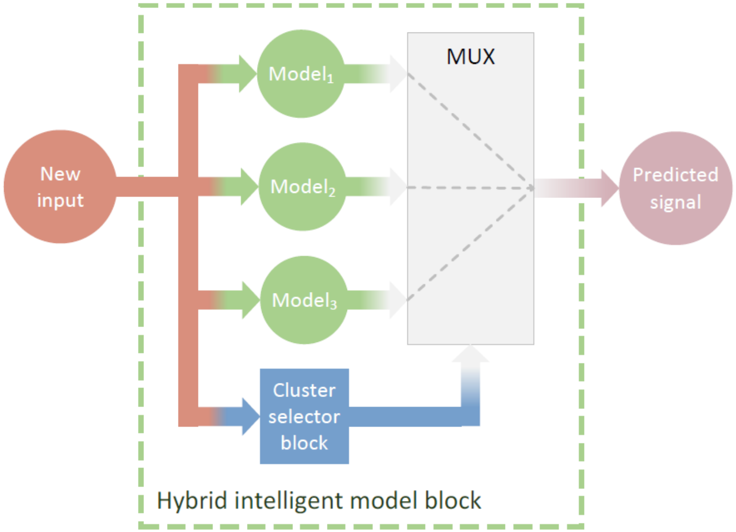

HYBRID INTELLIGENT MODEL FOR SOLAR ENERGY PREDICTION

Hybrid Intelligent Model for Solar Energy Prediction

- Case of Study (the same)

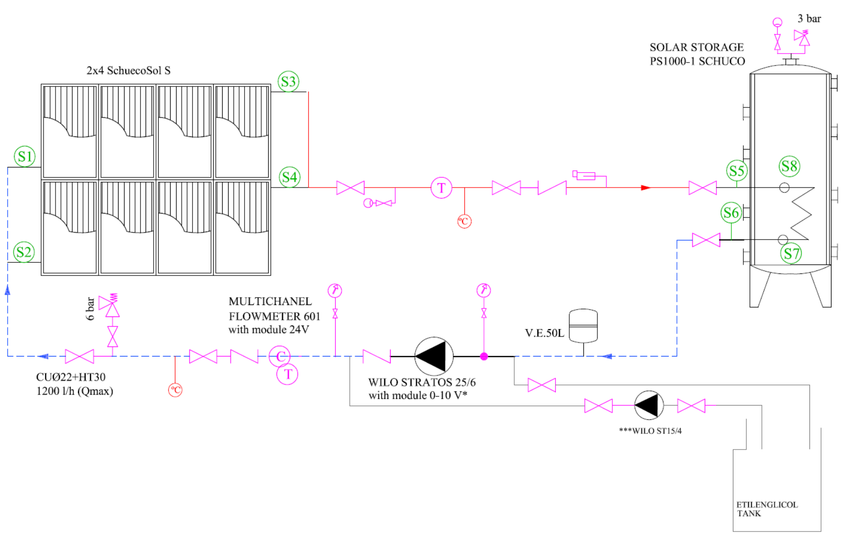

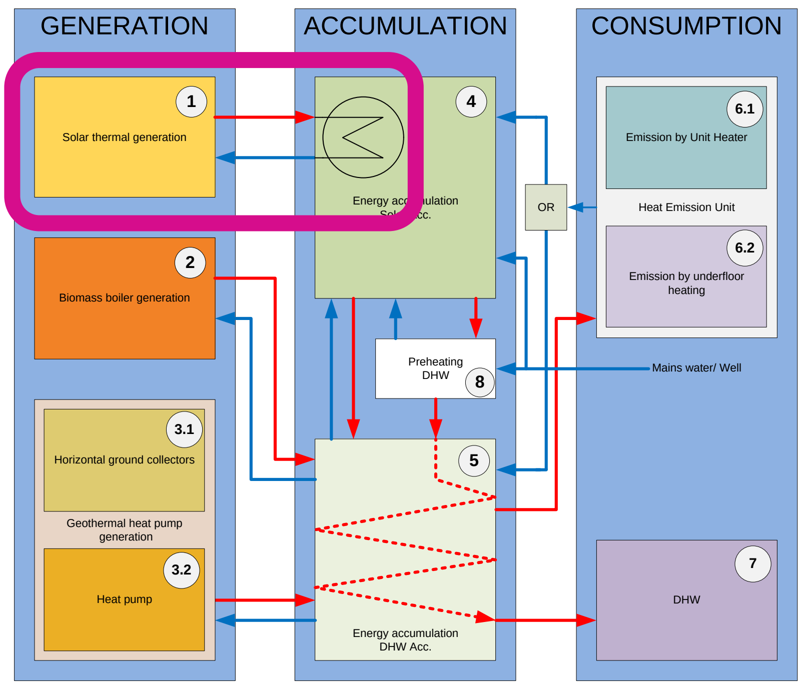

Hybrid Intelligent Model for Solar Energy Prediction

- The model approach

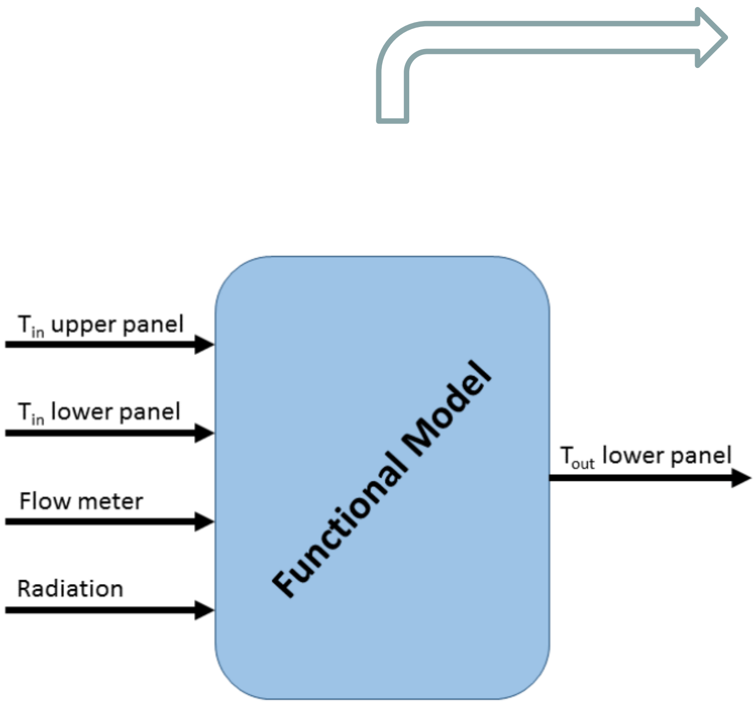

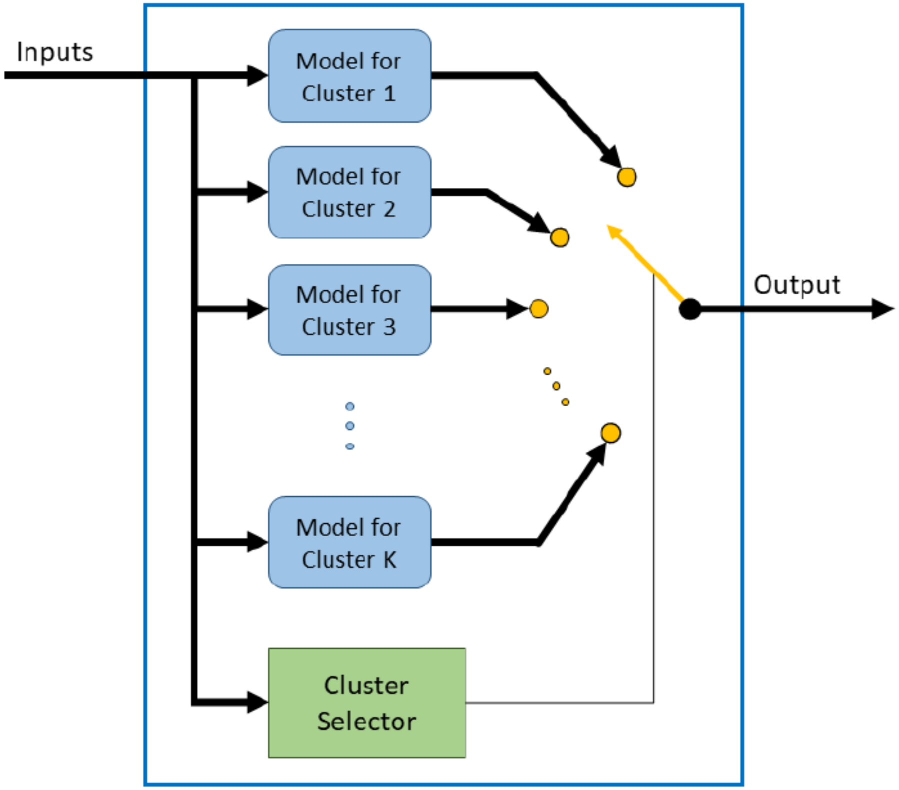

Hybrid Intelligent Model for Solar Energy Prediction

- Techniques:
  - K-Means
  - Artificial Neural Networks (MLP)
  - Polynomial Regression
  - Support Vector Machines for Regression

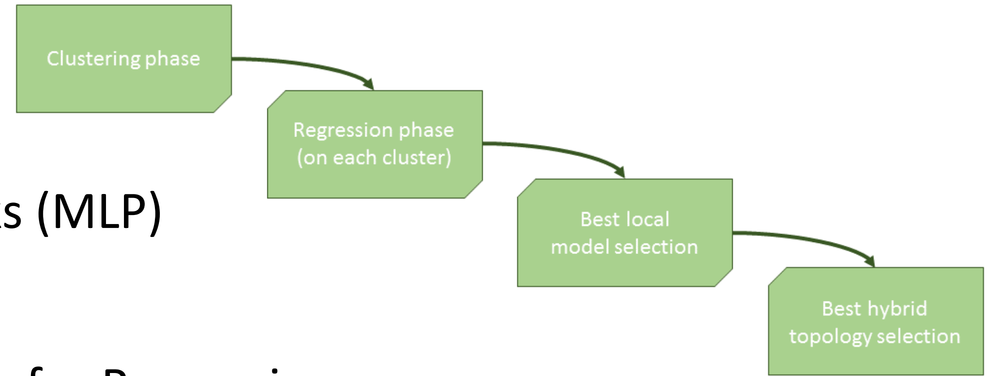

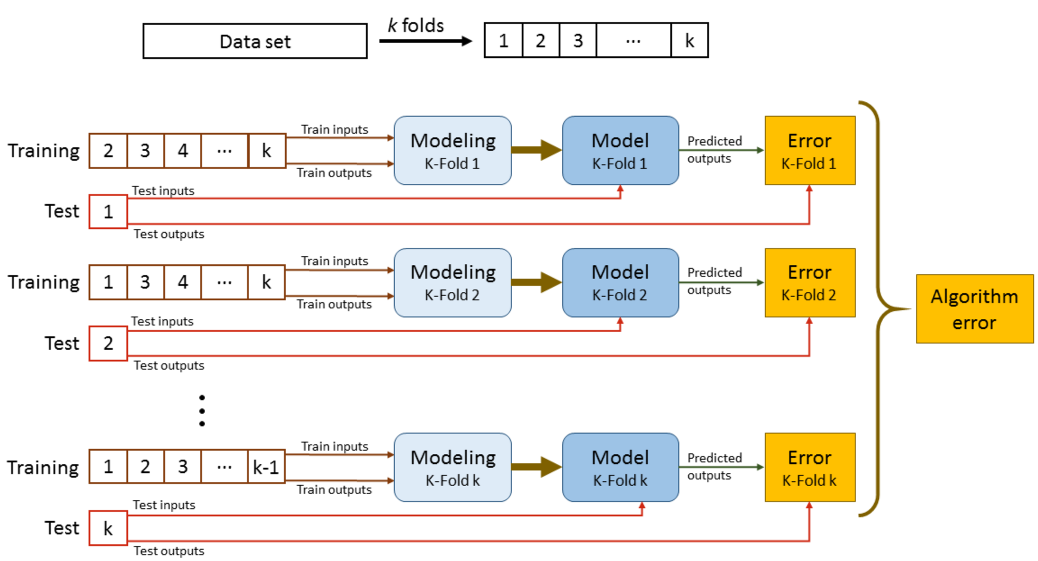

- Results:

Table 6. Mean squared error (MSE) for each individual hybrid model; all values $\times 10^{-4}$.

	Global	Hybrid Model (Local Models)								
		2	**3**	**4**	**5**	**6**	**7**	**8**	**9**	**10**
Cl-1	16.8972	3.1161	1.0321	5.9668	6.2402	5.6794	6.3455	6.3268	6.1555	5.9393
Cl-2		21.8021	9.8955	0.4348	6.9023	0.6041	9.0305	8.0789	9.4405	12.1097
Cl-3			26.6203	9.7590	0.3851	0.3093	0.5586	7.6646	7.6268	8.0194
Cl-4				26.2704	19.9626	7.4397	0.2725	0.5744	10.5137	10.7156
Cl-5					26.4265	21.2670	7.0769	0.2332	0.5387	11.0445
Cl-6						26.1993	22.3688	14.7125	0.2308	0.4686
Cl-7							25.9529	19.6236	15.8058	0.2294
Cl-8								31.8514	18.4699	10.7052
Cl-9									32.7775	25.8231
Cl-10										33.1709

Hybrid Intelligent Model for Solar Energy Prediction

- Results:

Table 5. Mean absolute error (MAE) for each individual hybrid model.

	Global	Hybrid Model (Local Models)								
		2	**3**	**4**	**5**	**6**	**7**	**8**	**9**	**10**
Cl-1	0.0278	0.0080	0.0060	0.0186	0.0199	0.0182	0.0190	0.0197	0.0196	0.0186
Cl-2		0.0346	0.0193	0.0044	0.0157	0.0053	0.0204	0.0192	0.0146	0.0143
Cl-3			0.0403	0.0194	0.0043	0.0037	0.0050	0.0143	0.0200	0.0185
Cl-4				0.0399	0.0326	0.0170	0.0037	0.0051	0.0182	0.0194
Cl-5					0.0398	0.0338	0.0148	0.0034	0.0050	0.0238
Cl-6						0.0397	0.0354	0.0269	0.0034	0.0047
Cl-7							0.0394	0.0337	0.0296	0.0034
Cl-8								0.0448	0.0321	0.0242
Cl-9									0.0455	0.0392
Cl-10										0.0463

- Results:

Table 7. Configuration for each individual hybrid model.

	Global	Hybrid Model (Local Models)								
		2	**3**	**4**	**5**	**6**	**7**	**8**	**9**	**10**
Cl-1	ANN-14	ANN-5	ANN-14	ANN-9	ANN-4	ANN-10	ANN-12	ANN-6	ANN-9	ANN-9
Cl-2		ANN-13	ANN-14	ANN-14	ANN-5	ANN-6	LS-SVR	LS-SVR	LS-SVR	LS-SVR
Cl-3			ANN-14	ANN-10	ANN-12	Poly-1	ANN-14	ANN-4	ANN-8	ANN-4
Cl-4				ANN-15	ANN-14	ANN-3	Poly-1	ANN-12	ANN-6	ANN-10
Cl-5					ANN-14	ANN-8	ANN-3	ANN-6	ANN-12	LS-SVR
Cl-6						ANN-15	ANN-9	ANN-8	ANN-6	ANN-10
Cl-7							ANN-14	ANN-10	LS-SVR	ANN-6
Cl-8								ANN-13	ANN-11	LS-SVR
Cl-9									ANN-14	ANN-11
Cl-10										ANN-10

Table 8. Error values for the different hybrid configurations.

	Global	Hybrid Model (Local Models)								
		2	**3**	**4**	**5**	**6**	**7**	**8**	**9**	**10**
MSE	0.0016	0.0016	0.0015	0.0015	0.0015	0.0015	0.0015	0.0015	0.0014	0.0014
MAE	0.0272	0.0270	0.0258	0.0257	0.0258	0.0259	0.0259	0.0255	0.0247	0.0250
NMSE	0.1116	0.1095	0.1038	0.1023	0.1036	0.1030	0.1047	0.1005	0.0977	0.1001

Hybrid Intelligent Model for Solar Energy Prediction

- Comparison between global and hybrid models:

Table 9. Hybrid intelligent approach vs. global models with different regression algorithms.

	Hybrid Model with 9 Clusters	Global Models								
		LS-SVR	**Poly-1**	**Poly-2**	**ANN-3**	**ANN-5**	**ANN-6**	**ANN-9**	**ANN-11**	**ANN-13**
MSE	0.0014	0.0018	0.0024	0.0025	0.0022	0.0020	0.0020	0.0020	0.0018	0.0017
MAE	0.0247	0.0283	0.0324	0.0314	0.0320	0.0304	0.0298	0.0288	0.0282	0.0279
NMSE	0.0977	0.1161	0.1489	0.1571	0.1415	0.1279	0.1240	0.1277	0.1117	0.1073

Hybrid Intelligent Model for Solar Energy Prediction

- Graphical Results:

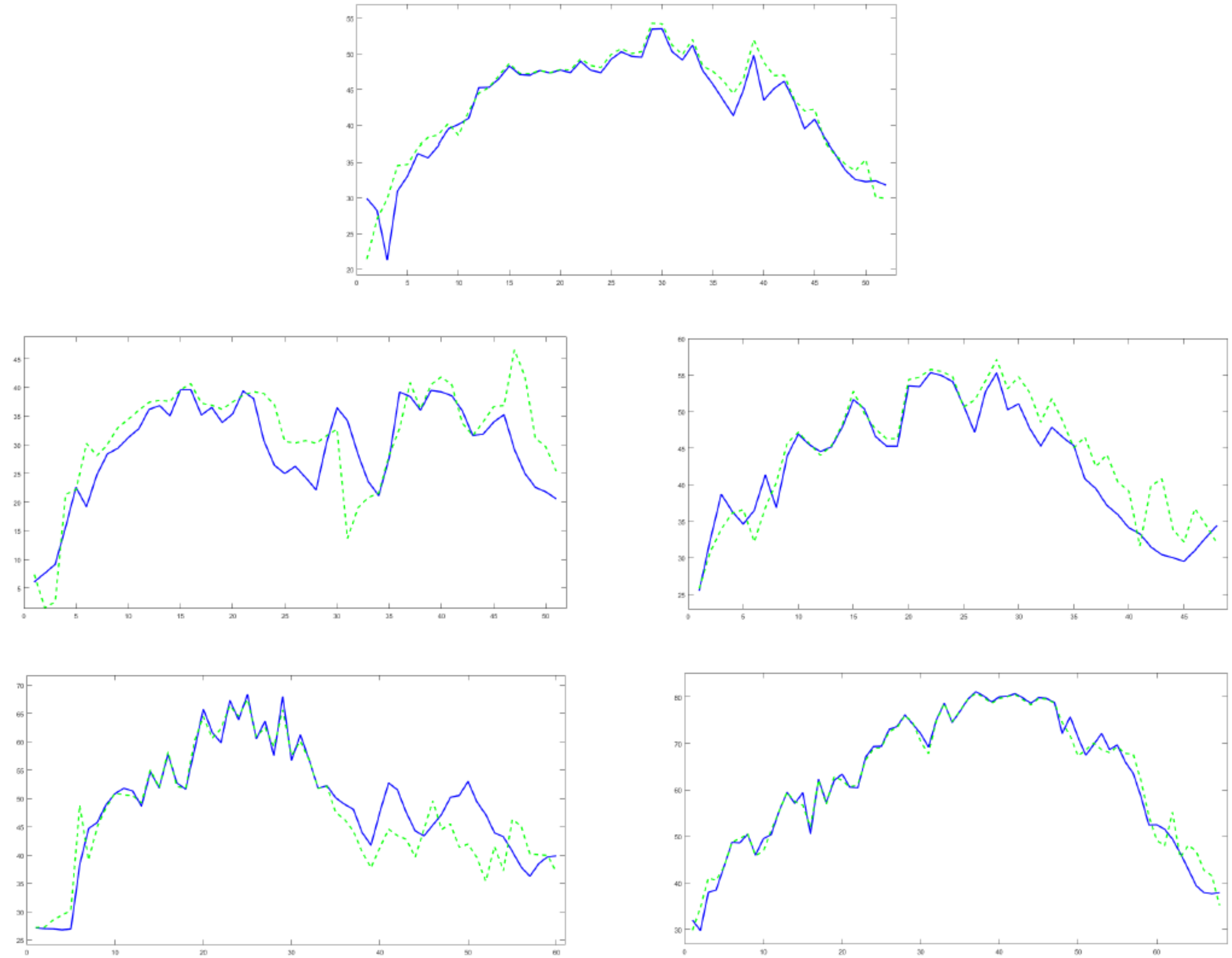

GEOTHERMAL HEAT EXCHANGER MODELING

Geothermal Heat Exchanger Modeling

- Case of Study

Geothermal Heat Exchanger Modeling

- Case of Study

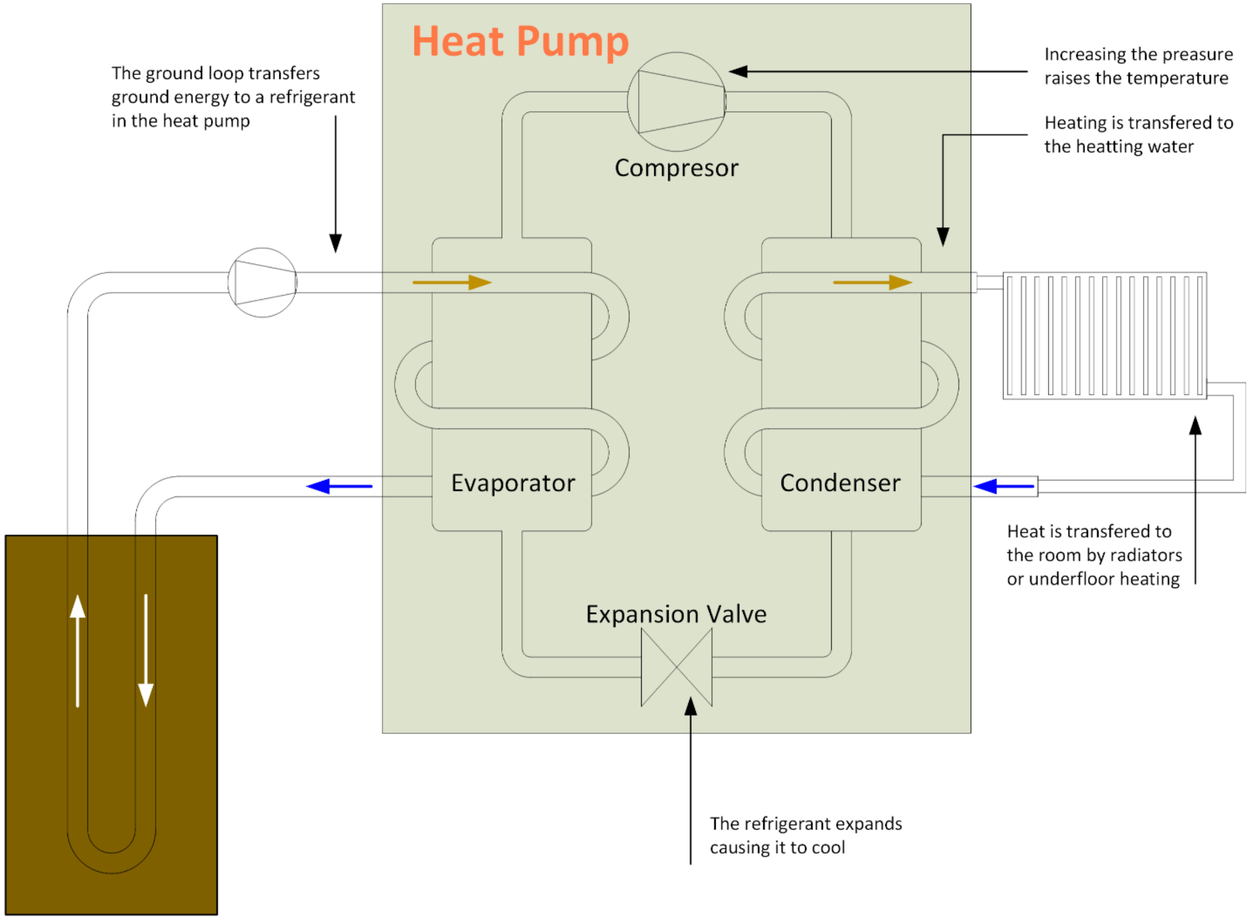

Geothermal Heat Exchanger Modeling

- Case of Study

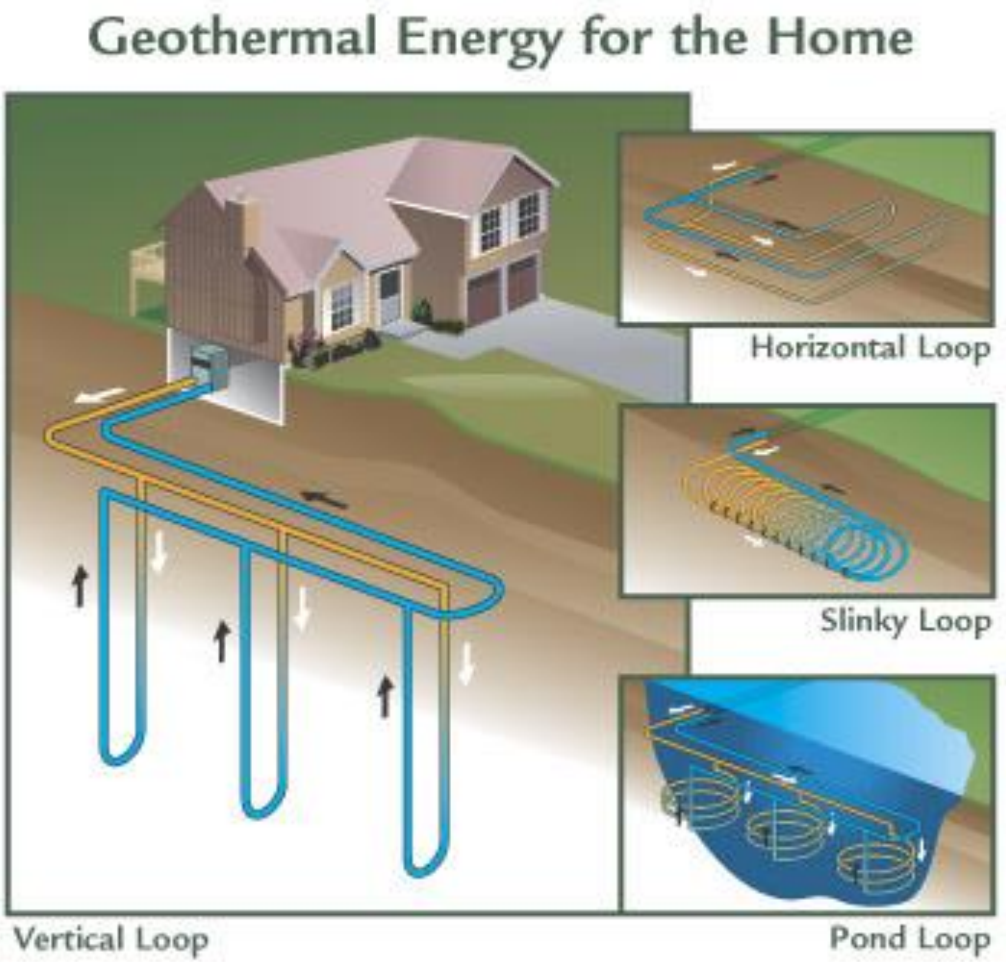

Geothermal Heat Exchanger Modeling

- Case of Study

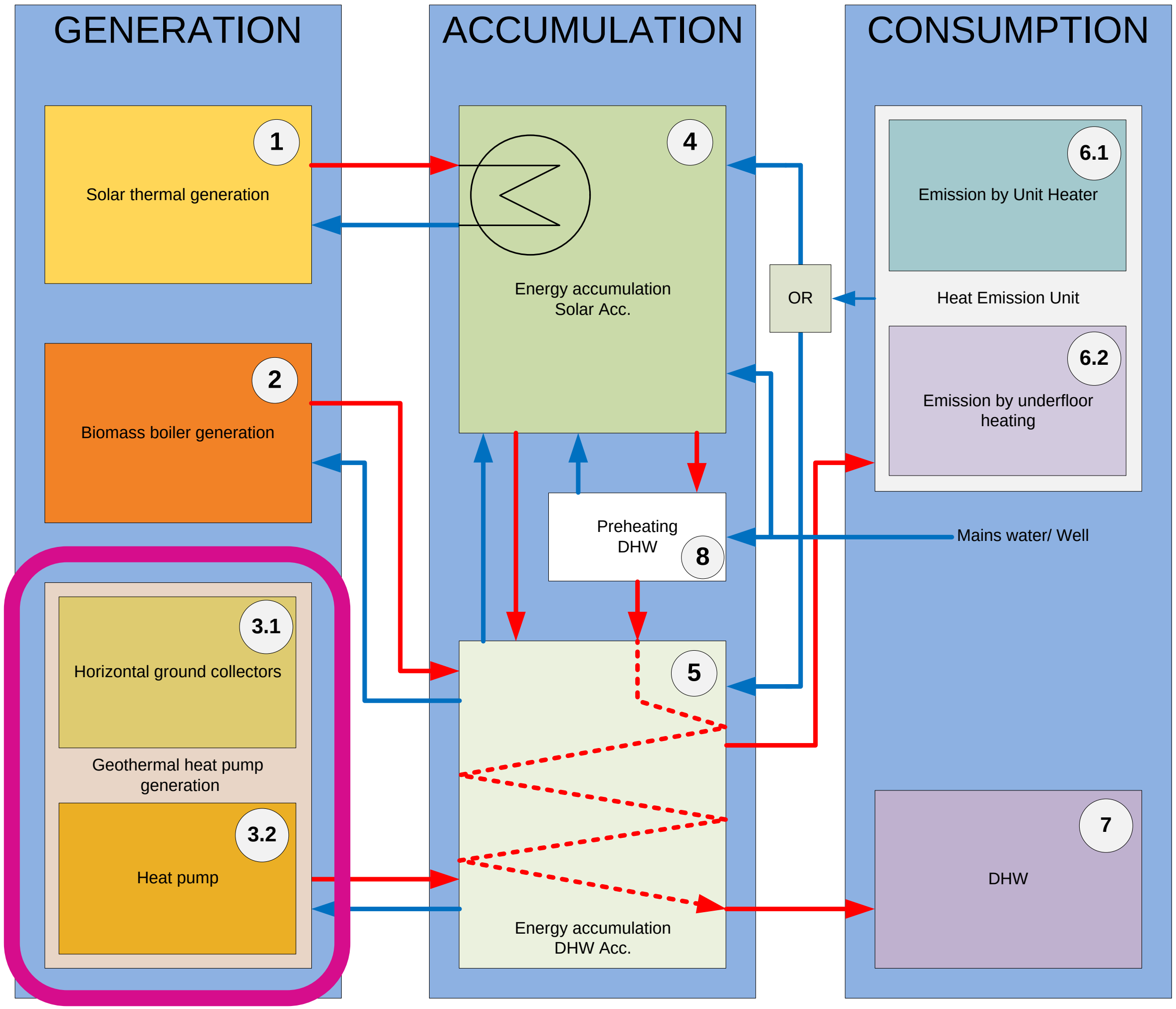

Geothermal Heat Exchanger Modeling

- Case of Study

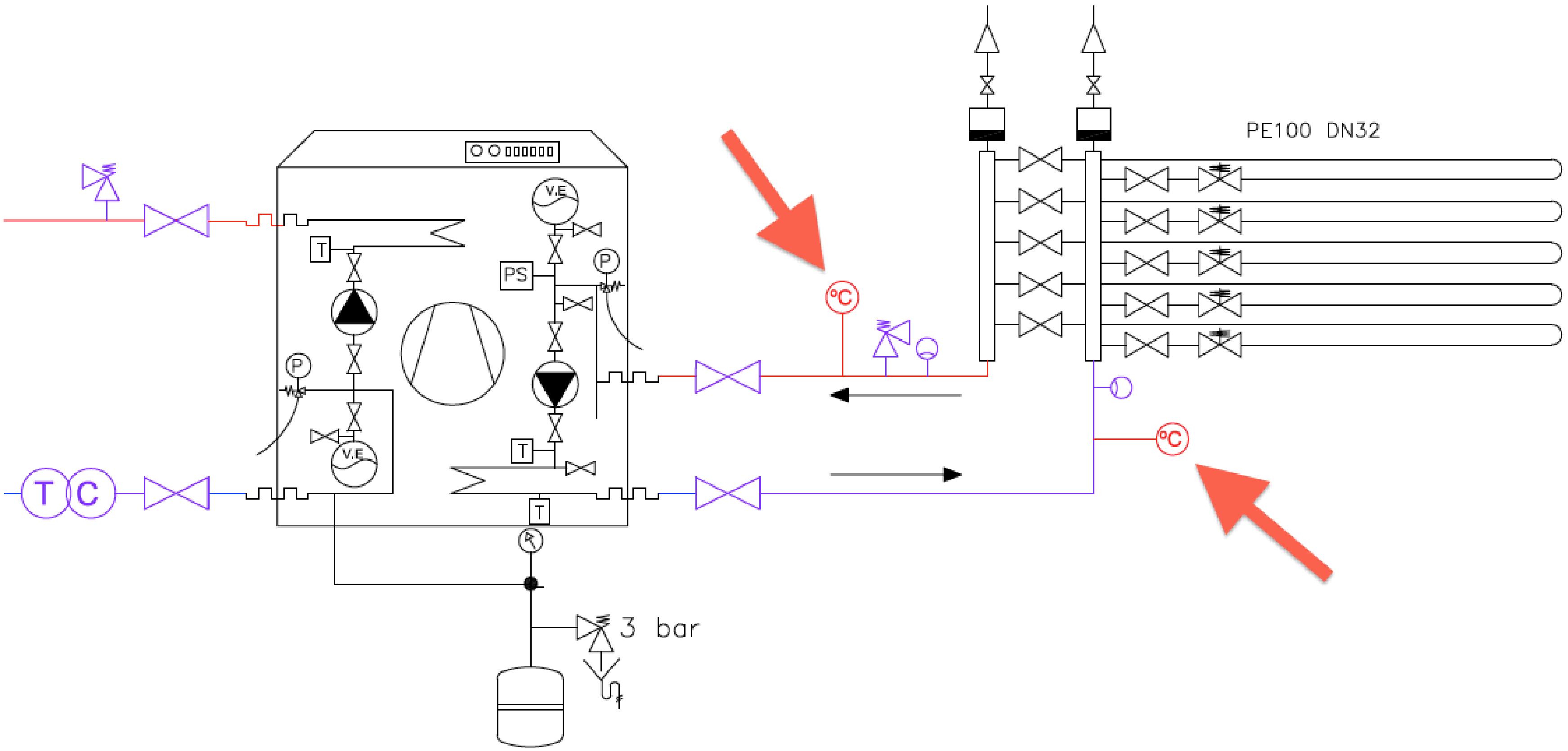

Geothermal Heat Exchanger Modeling

- Case of Study

The heat pump

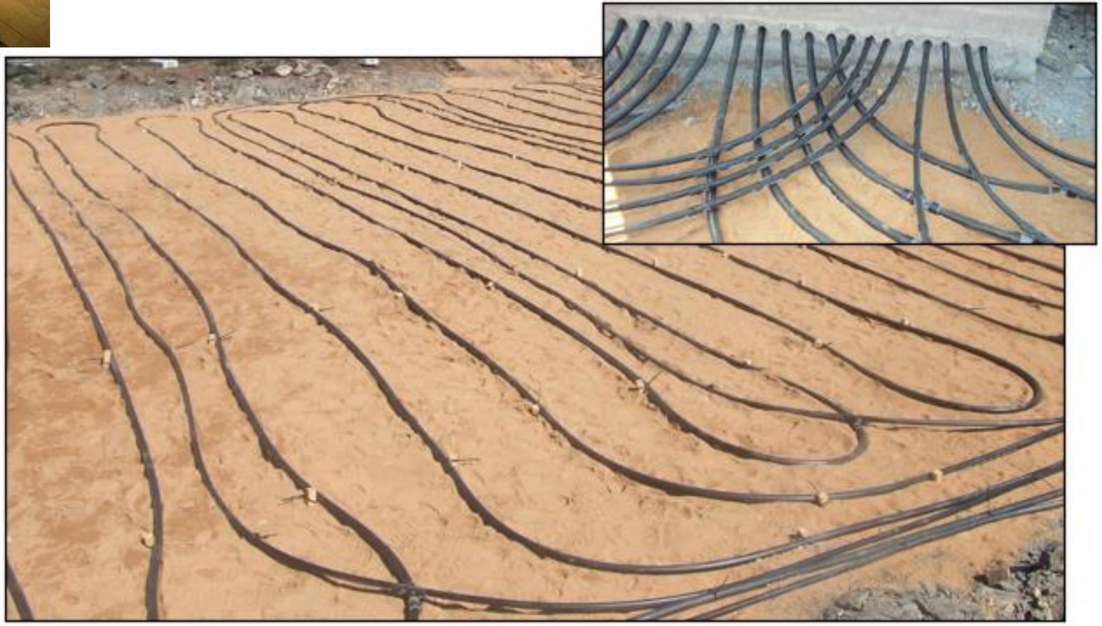

The horizontal heat exchanger

Geothermal Heat Exchanger Modeling

- Case of Study

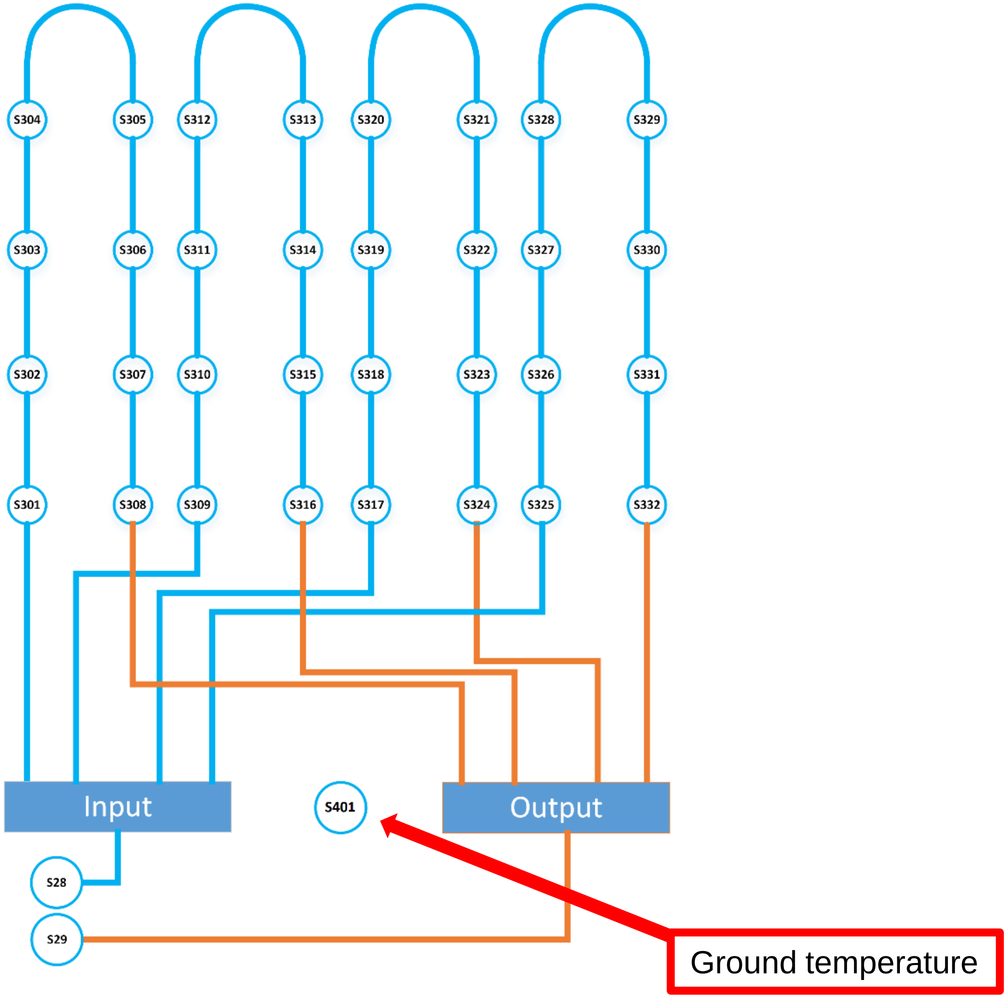

The horizontal heat exchanger schema

Geothermal Heat Exchanger Modeling

- Dataset and its processing
  - It consist on the temperatures at each sensor during one year.
  - There were missing data and errors during the acquisition.
  - Totally, there were 52,705 samples.
  - The dataset was filtered and cleaned to discard the erroneous data.
  - The dataset have 52,699 samples after conditioning.

Geothermal Heat Exchanger Modeling

- Dataset understanding.
  - The sensors are inside the house.
  - This measurements must be corrected.
  - The difference between the input and the output is due to the energy extracted from the ground.

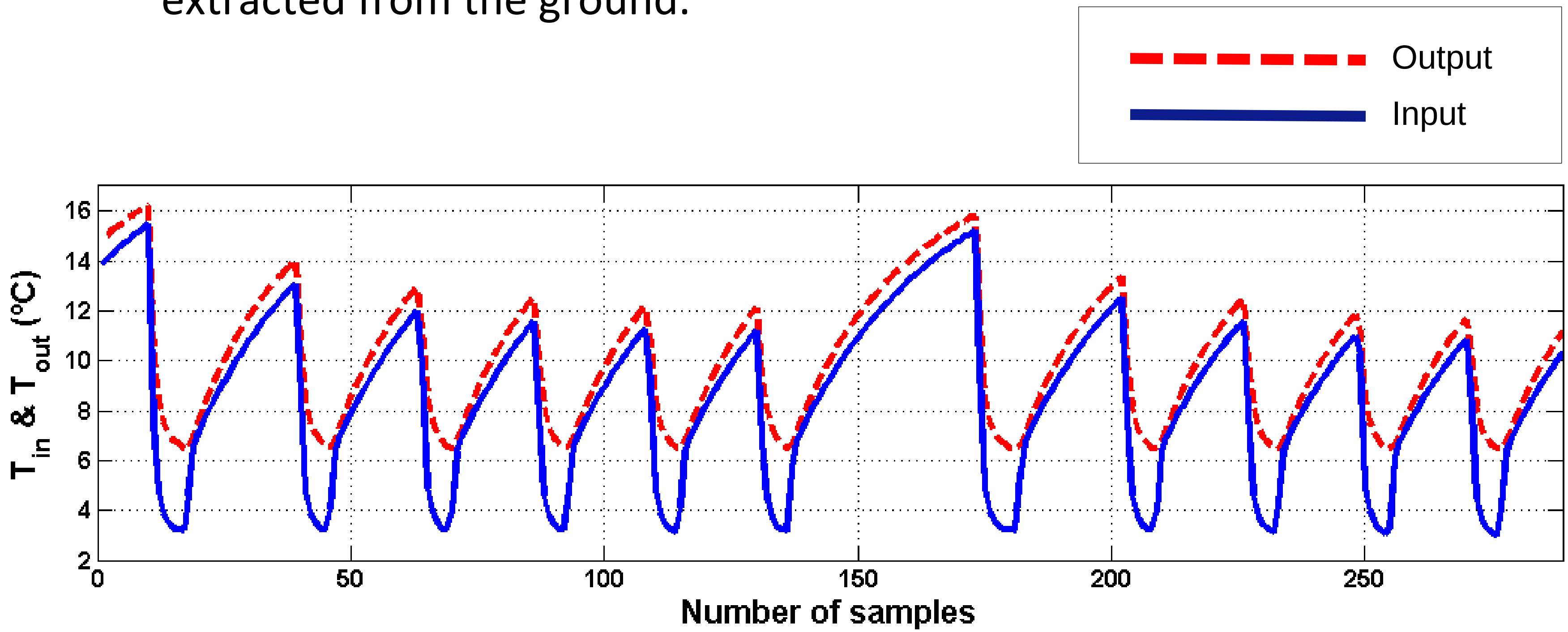

Geothermal Heat Exchanger Modeling

- Dataset understanding.
  - This dataset was corrected by fixing the maximum temperature to the outside one.

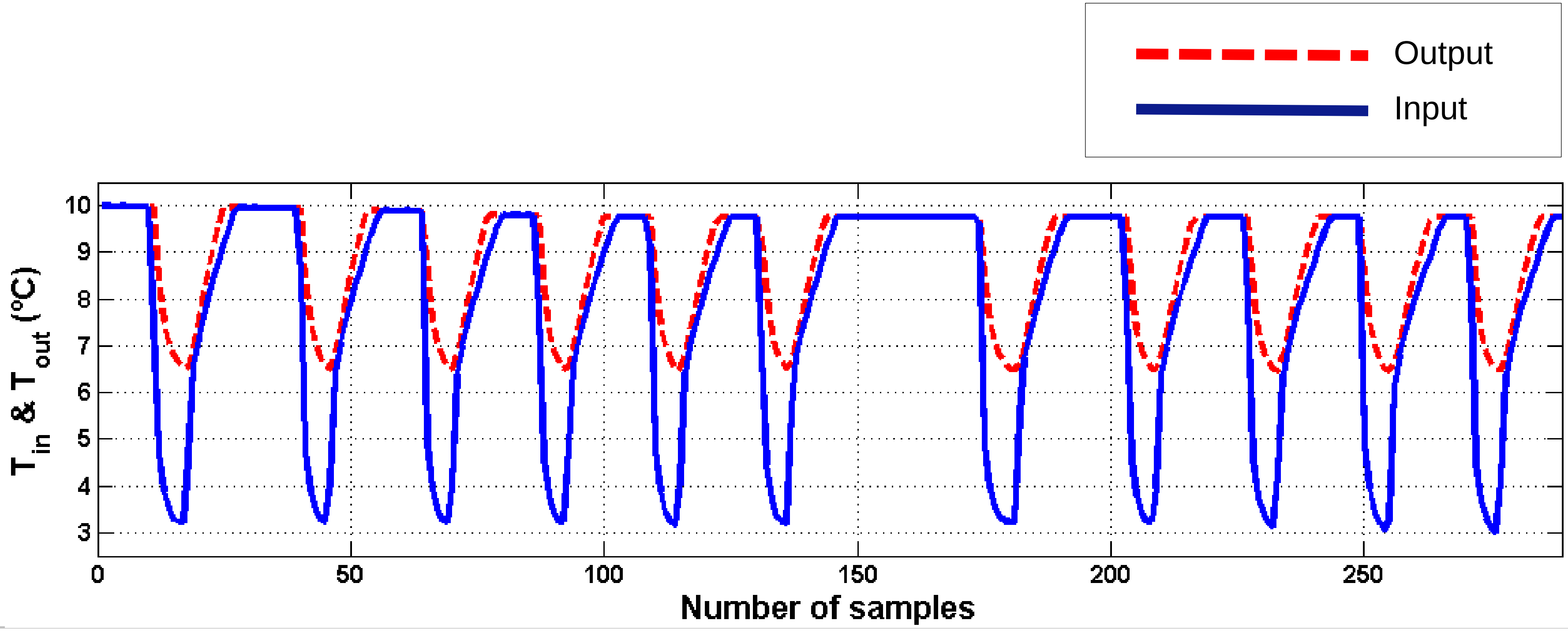

Geothermal Heat Exchanger Modeling

- Dataset understanding.
  - A specific cycle was insulated for showing the performance.
  - More or less 4ºC are obtained.
  - The energy obtained from the ground decrease with time when the system is in operation.

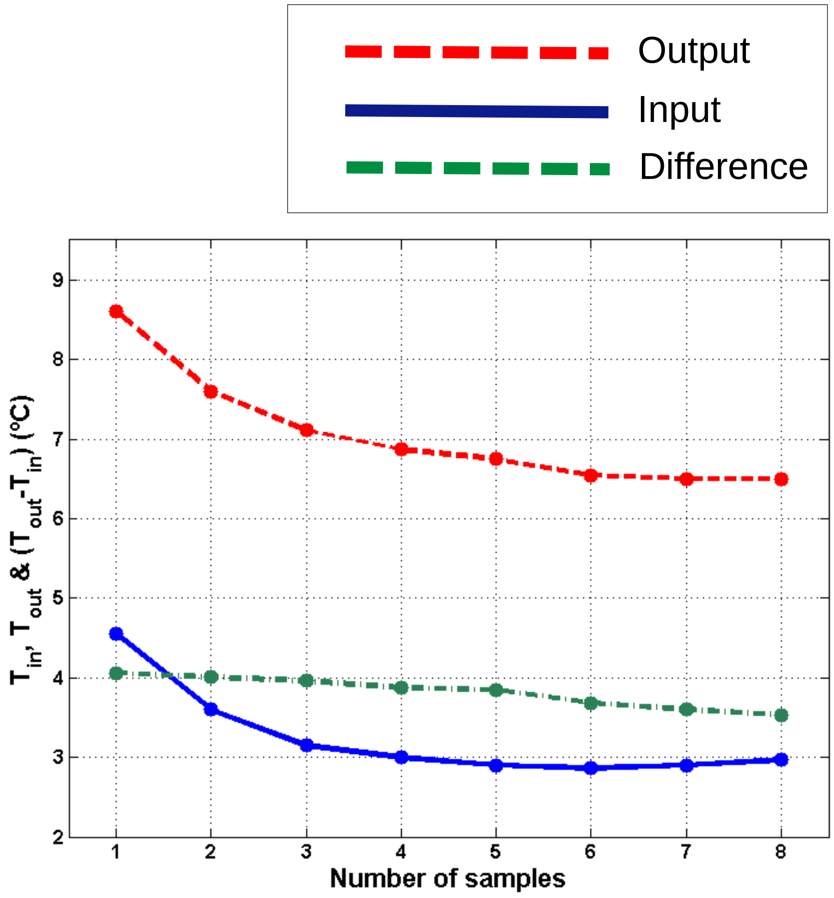

Geothermal Heat Exchanger Modeling

- Dataset understanding.
  - This figure show a full working cycle for the Heat Pump since its put in operation
  - It is the difference between the output and input of the geothermal heat exchanger.
  - It is possible to appreciate the fast increase of the temperature at the beginning of the cycle.
  - it is possible to conclude, the temperature value is almost constant after more or less twenty minutes working.

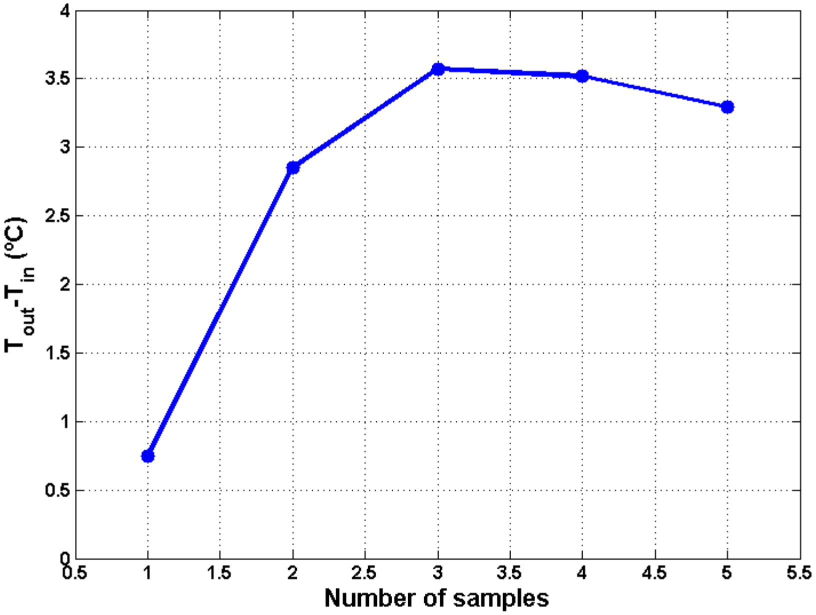

Geothermal Heat Exchanger Modeling

- Dataset understanding.
  - If the heat exchanger is running during more time (the triple), the decreasing trend of the extracting temperature descends.
  - For the five working cycles (chosen randomly), the increased temperature has the same trend.
  - The main difference is the maximum temperature attained.
  - The reason is due that the different graphs are from different seasons.
  - Then, the performance does not depend of the weather directly.

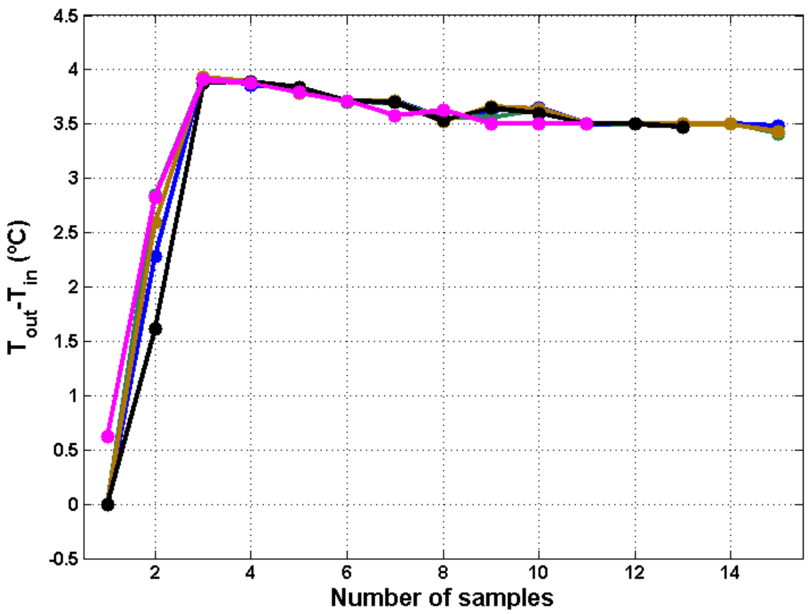

Geothermal Heat Exchanger Modeling

- Objective → Predict 'Ground Temperature' value

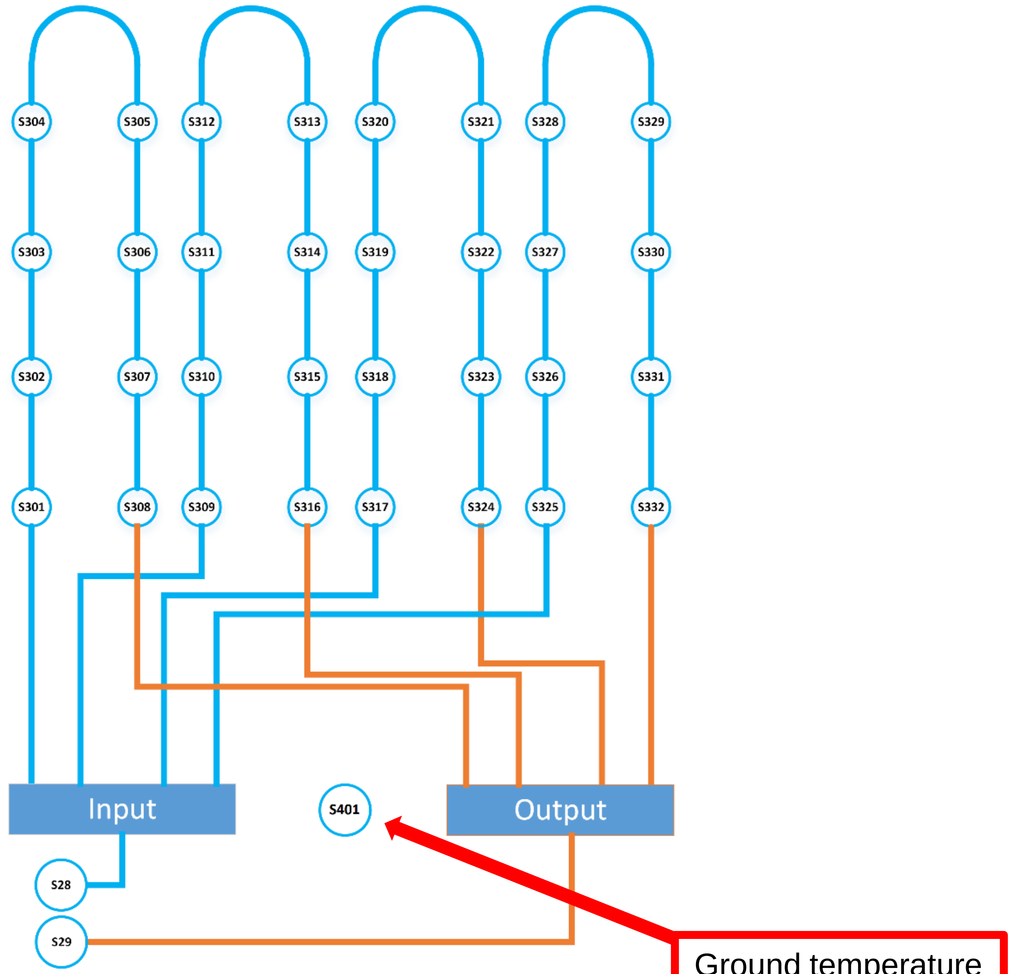

The horizontal heat exchanger schema

Geothermal Heat Exchanger Modeling

- The model approach

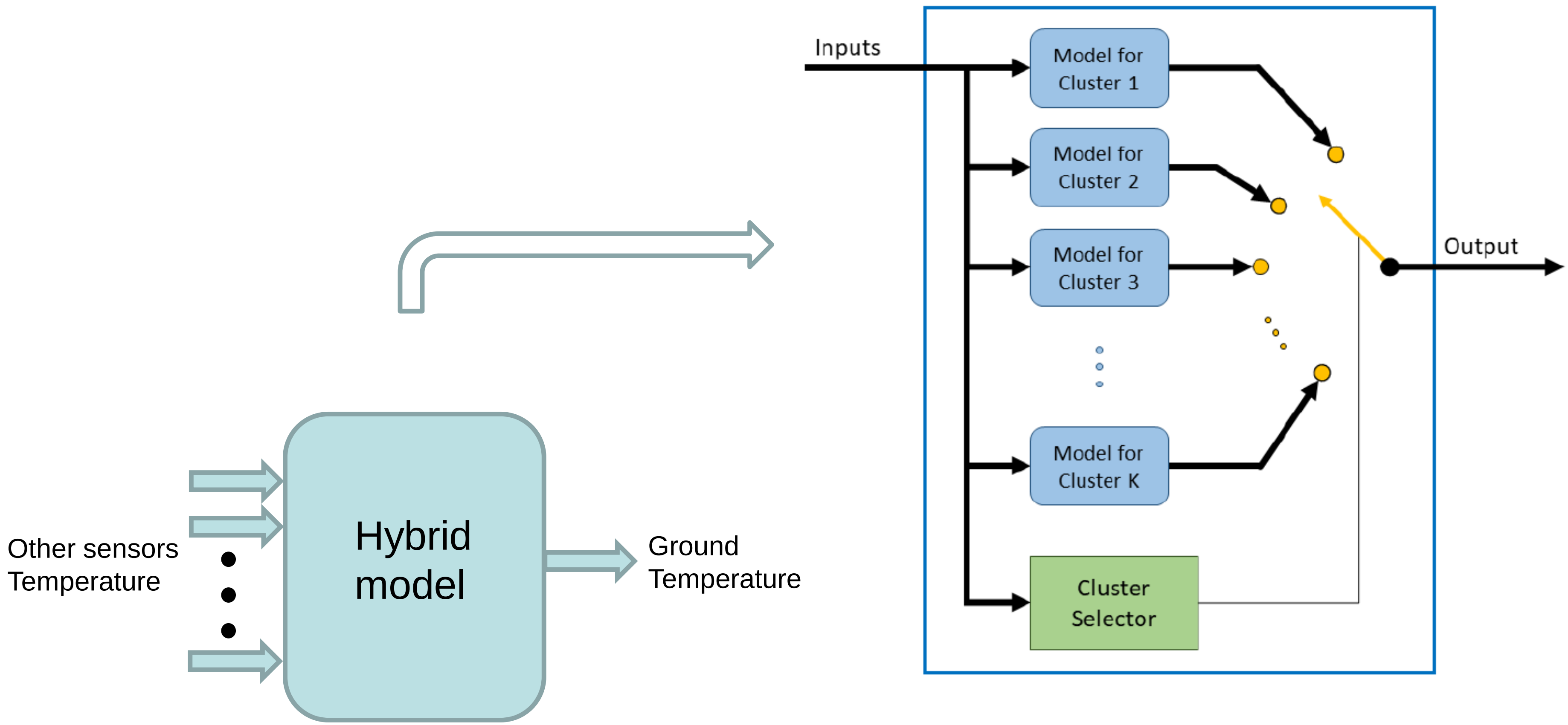

Geothermal Heat Exchanger Modeling

- Techniques:
  - K-Means
  - Artificial Neural Networks (MLP)
  - Polynomial Regression
  - Support Vector Machines for Regression

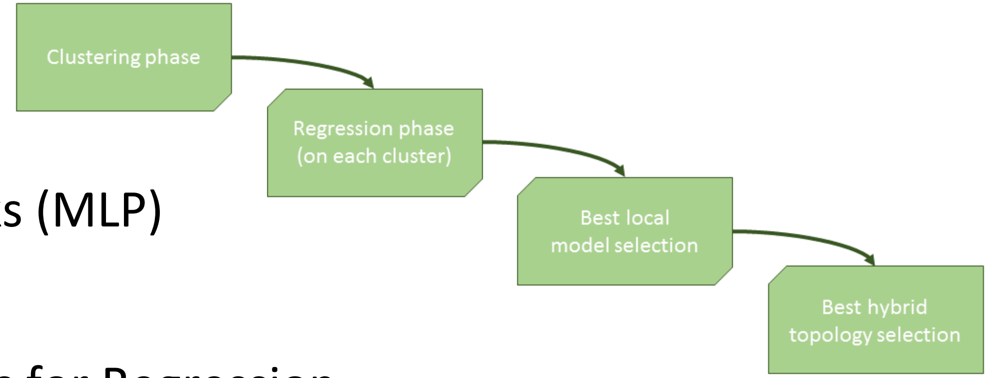

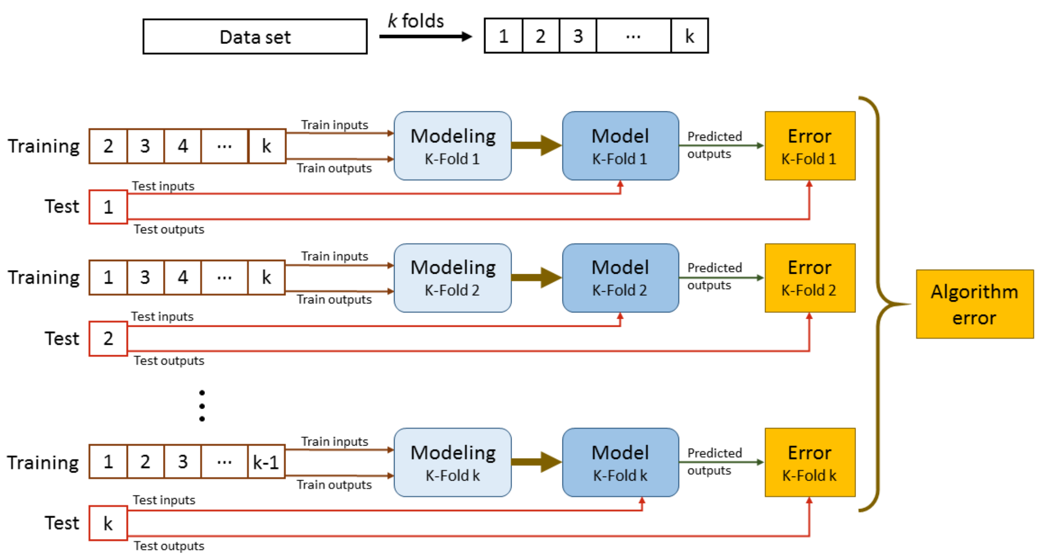

Geothermal Heat Exchanger Modeling

- Results:

Clusters quantity	Cluster number	Train	Test	Total
No clusters		35,133	17,566	52,699
3 Clusters				
	1	10,244	5077	15,321
	2	14,714	7369	22,083
	3	10,175	5120	15,295
4 Clusters				
	1	9714	4874	14,588
	2	6507	3257	9764
	3	12,433	6229	18,662
	4	6479	3206	9685
5 Clusters				
	1	3443	1722	5165
	2	6441	3184	9625
	3	5954	2981	8935
	4	12,422	6227	18,649
	5	6873	3452	10,325
6 Clusters				
	1	6870	3450	10,320
	2	3430	1646	5076
	3	4842	2557	7399
	4	10,536	5286	15,822
	5	4473	2217	6690
	6	4982	2410	7392
7 Clusters				
	1	4660	2454	7114
	2	7066	3548	10,614
	3	3694	1891	5585
	4	4980	2405	7385
	5	3430	1646	5076
	6	6870	3450	10,320
	7	4433	2172	6605

MSE for different regression techniques—4 clusters.

Cluster no	Train samples	Test samples	MSE		
			ANN-MLP	Polynomial	LS-SVR
Cluster 1	9714	4874	0.00632	0.00882	0.00678
Cluster 2	6507	3257	0.00493	0.00926	0.00513
Cluster 3	12,433	6229	0.00613	0.01034	0.00671
Cluster 4	6479	3206	0.00598	0.00974	0.00632

MSE comparison.

Model type	No of clusters	MSE
Global model		0.0221
Local models	3 Clusters	0.0076
	4 Clusters	0.0059
	5 Clusters	0.0069
	6 Clusters	0.0063
	7 Clusters	0.0121

Geothermal Heat Exchanger Modeling

- Conclusions:
  - All the achieved configurations of the model have a nice performance.
  - The better performance correspond to one of the hybrid configuration.
  - There are multiple reasons that could affect to the geothermal heat exchanger.

ANOMALY DETECTION BASED ON VIRTUAL SENSORS

Anomaly detection based on virtual sensors

- Fundamentals
  - The virtual sensor concept.
  - Why anomaly detection/fault detection?

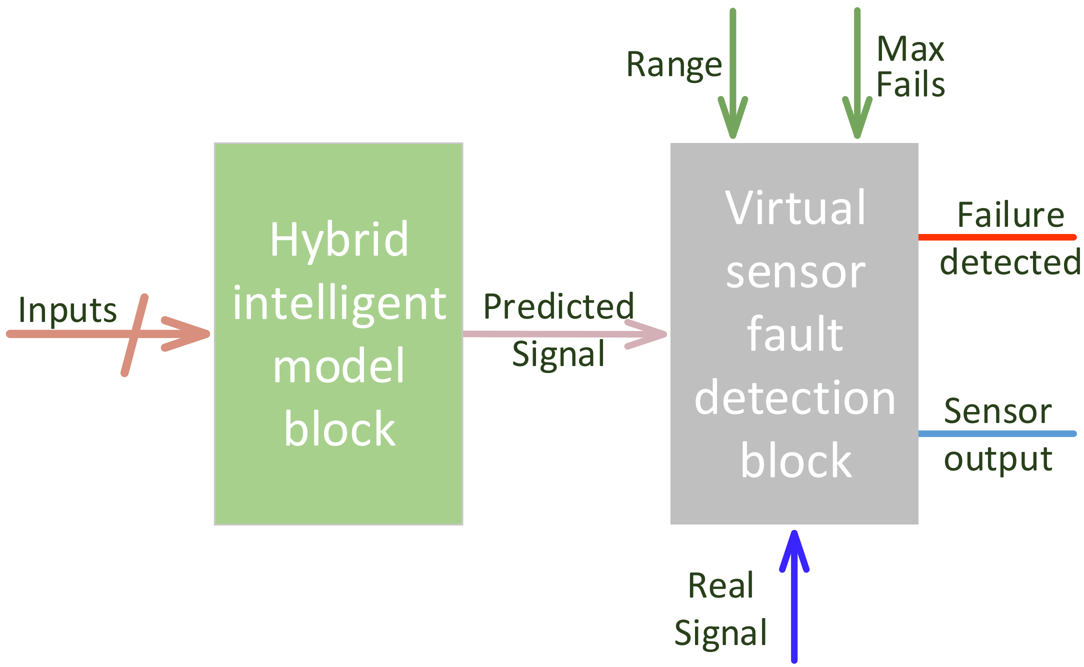

Anomaly detection based on virtual sensors

- Implementation
  - Hybrid intelligent model block.
    - Modeling process.
      - > Clustering.
      - > Modeling.
      - > Validation.
      - > Best configuration.

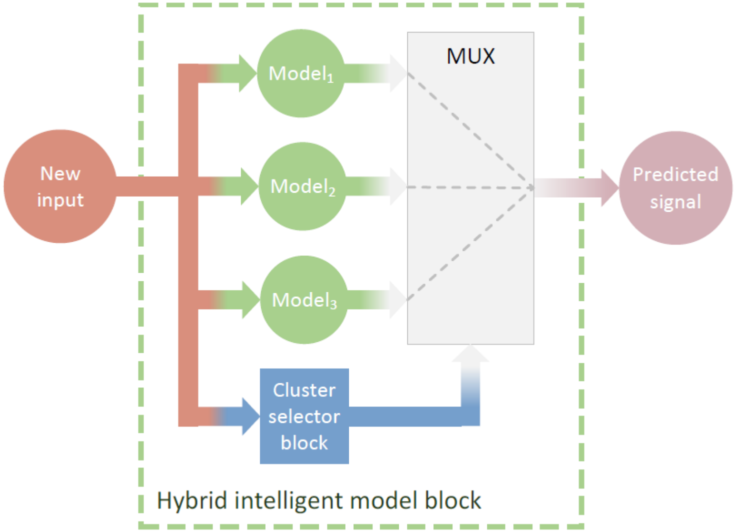

Anomaly detection based on virtual sensors

- Implementation
  - Virtual sensor fault detection block.
    - **Fault block.**
    - Counter block.
    - Output selector block.

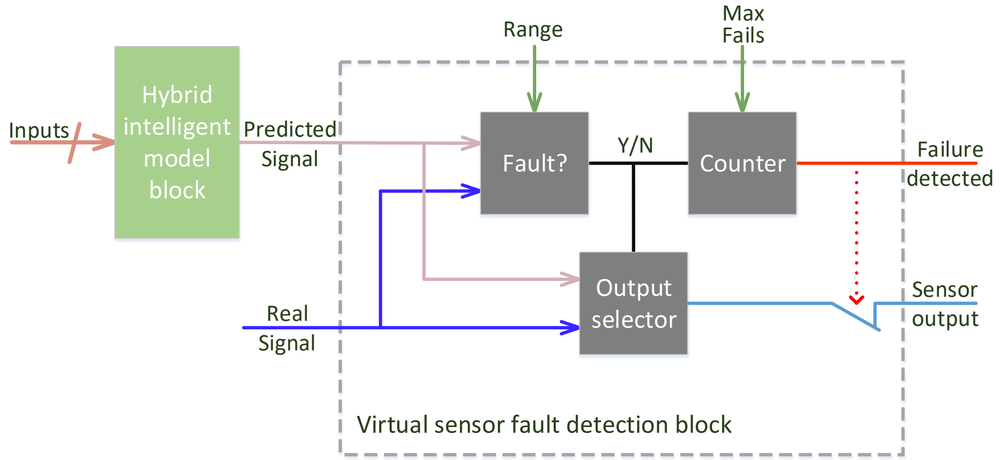

Anomaly detection based on virtual sensors

- Implementation
  - Virtual sensor fault detection block.
    - Fault block.
    - **Counter block.**
    - Output selector block.

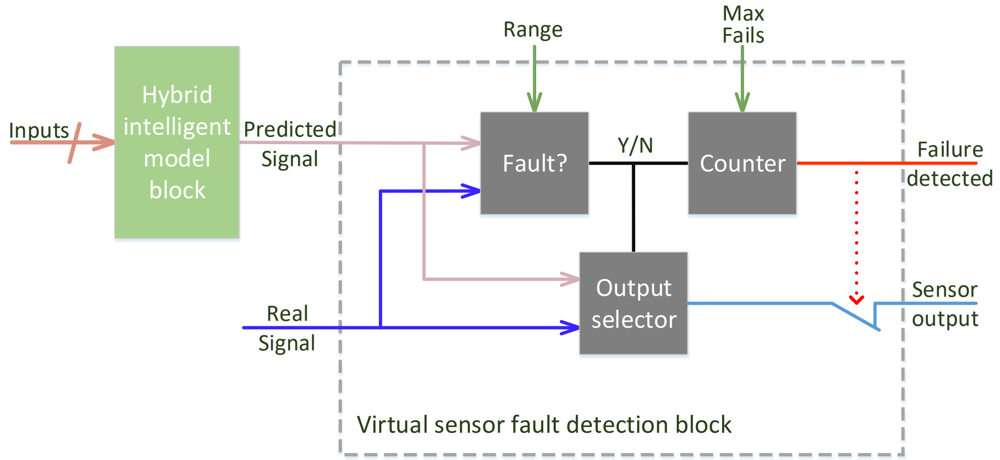

Anomaly detection based on virtual sensors

- Implementation
  - Virtual sensor fault detection block.
    - Fault block.
    - Counter block.
    - **Output selector block.**

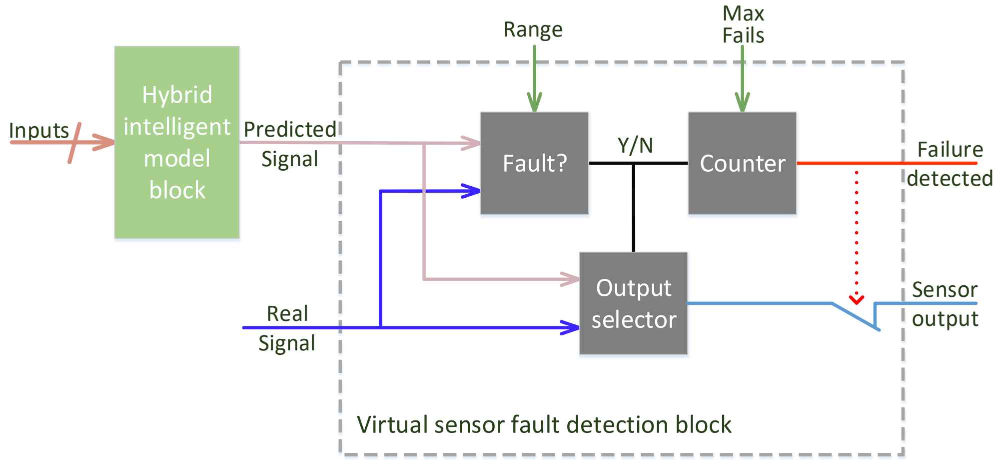

GEOTHERMAL HEAT EXCHANGER ANOMALY DETECTION BASED ON VIRTUAL SENSORS

Geothermal Heat Exchanger Anomaly Detection Based on Virtual Sensors

- Case of Study

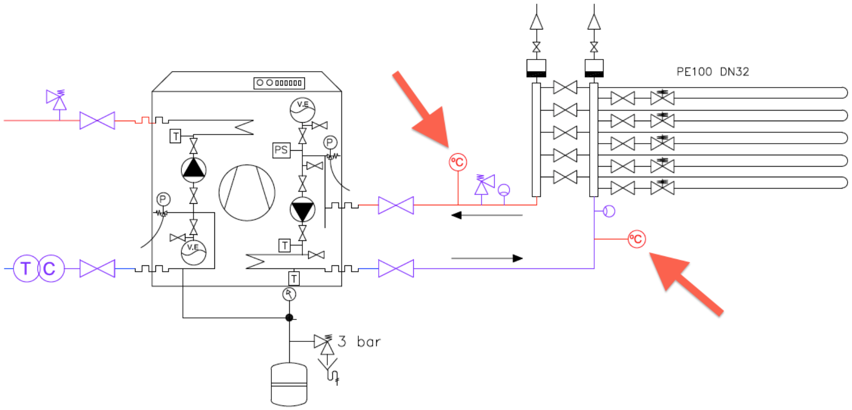

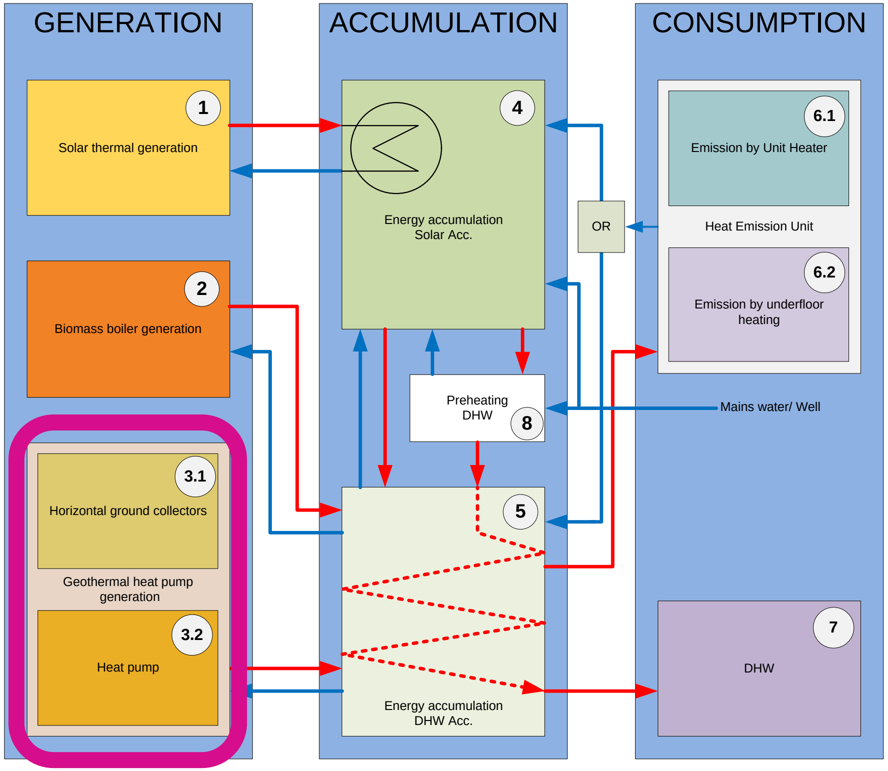

Geothermal Heat Exchanger Anomaly Detection Based on Virtual Sensors

- Objective → Anomaly detection of S-315 sensor

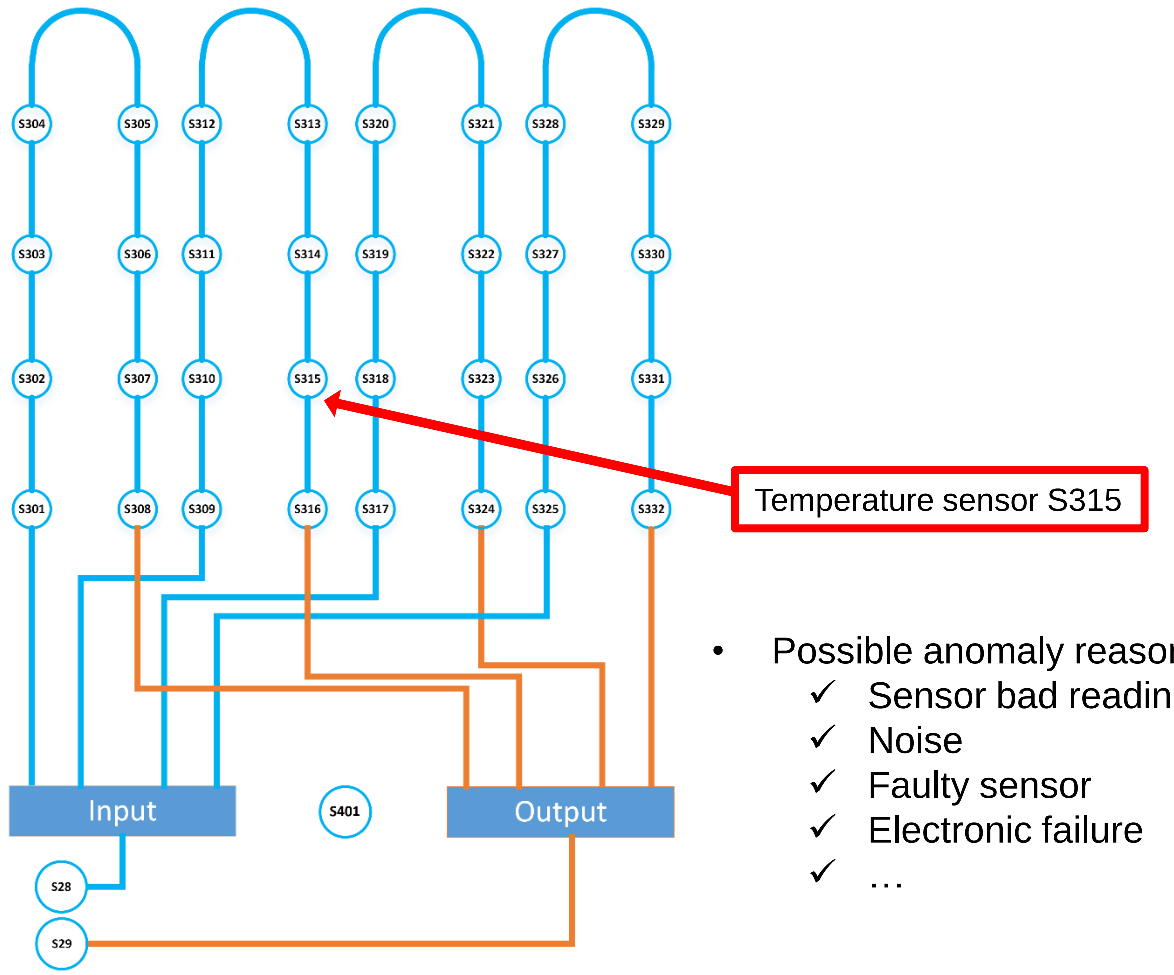

The horizontal heat exchanger schema

- Possible anomaly reasons:
  - ✓ Sensor bad reading
  - ✓ Noise
  - ✓ Faulty sensor
  - ✓ Electronic failure
  - ✓ …

Geothermal Heat Exchanger Anomaly Detection Based on Virtual Sensors

- The approach

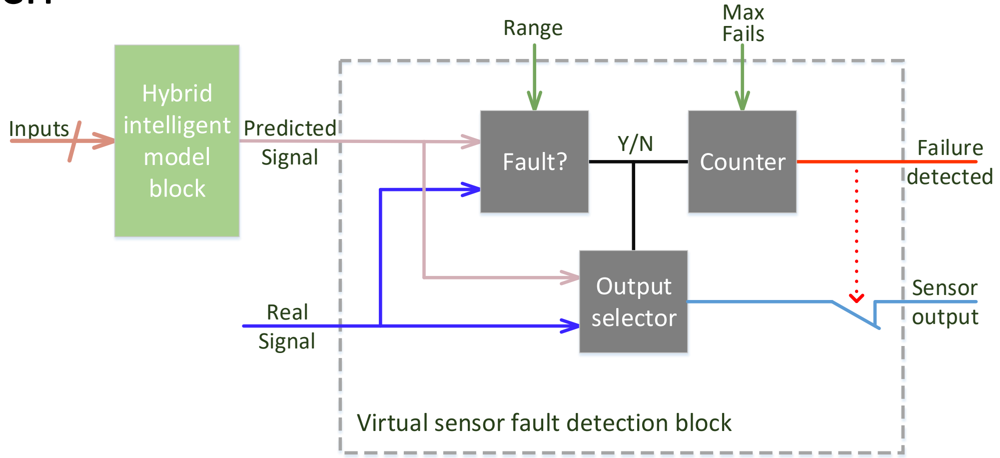

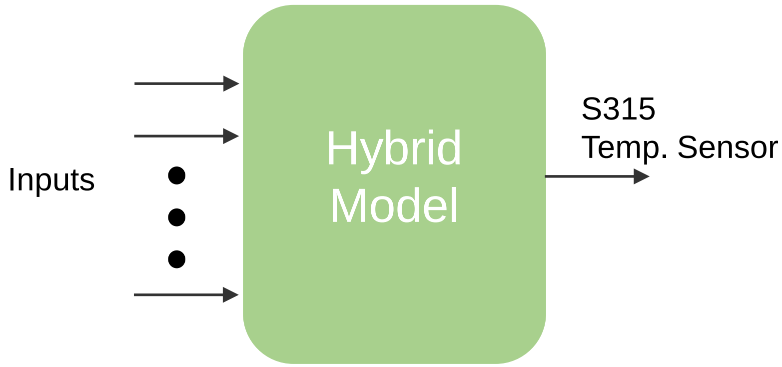

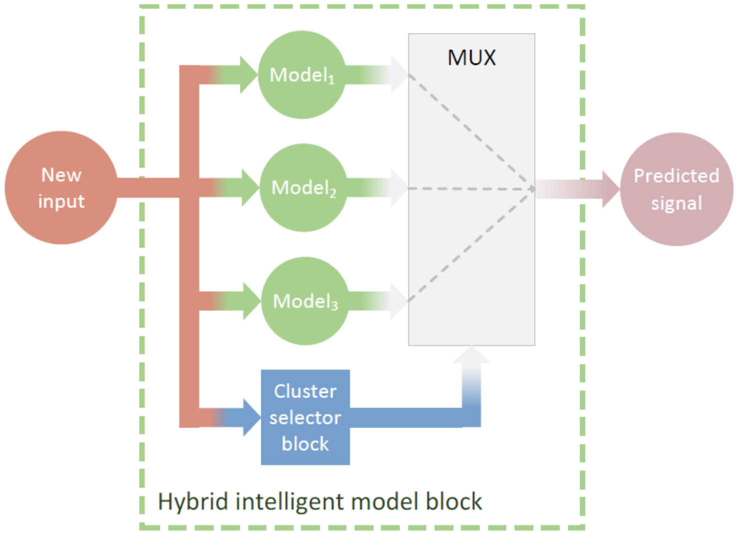

Geothermal Heat Exchanger Anomaly Detection Based on Virtual Sensors

- The hybrid model inputs:
  - Experiment A: Prediction of sensor S-315 based on S-309 to S-316 signals
  - Experiment B: Prediction of sensor S-315 based on S-309 to S-316 signals and their previous states
  - Experiment C: Prediction of sensor S-315 based on S-309 to S-316 signals and S-315 previous state
  - Experiment D: Prediction of sensor S-315 based on S-309 to S-316 signals, their previous states, and S-315 previous state

Geothermal Heat Exchanger Anomaly Detection Based on Virtual Sensors

- The contemplated regression techniques:
  - Shallow Neural Networks (MLP Advanced)
  - K-Nearest Neighbors
  - Adaptive Boosting
  - Random Decision Forests
  - Extremely Randomized Trees
  - Gradient Boosting
- Two kid of models with them:
  - Global models: In this case the whole data set is used for training a single regressor.
  - Hybrid models: In this case, the data set is split into two groups in accordance to day and night criteria.

Geothermal Heat Exchanger Anomaly Detection Based on Virtual Sensors

Error	Experiment	ET	GB	MLP	RF	AB	K-NN
LMLS	A	**2.4**	24.4	6.0	3.7	2.66	4.76
	B	**2.4**	21.2	6.7	3.5	3.16	4.76
	C	**2.6**	21.2	4.5	3.0	2.87	4.76
	D	**2.3**	16.6	18.7	3.2	3.26	4.76
MAE	A	**243.1**	880.6	495.3	280.3	263.76	353.77
	B	**240.1**	868.9	620.1	300.8	317.70	353.77
	C	**249.5**	821.5	414.9	280.7	277.65	353.77
	D	**243.5**	768.2	855.9	283.5	336.57	353.77
MAPE	A	**29.2**	106.0	59.9	33.7	31.72	42.62
	B	**28.9**	104.6	74.9	36.2	38.24	42.62
	C	**30.0**	98.9	50.1	33.8	33.40	42.62
	D	**29.3**	92.5	103.2	34.1	40.52	42.62
MSE	A	**4.8**	48.8	12.0	7.4	5.32	9.53
	B	**4.9**	42.5	13.4	7.0	6.33	9.53
	C	**5.2**	42.5	9.0	6.1	5.75	9.53
	D	**4.6**	33.2	37.5	6.3	6.51	9.53
NMSE	A	508.4	535.7	979.6	370.6	572.03	**108.90**
	B	527.9	570.0	250.6	320.7	540.69	**108.90**
	C	561.2	569.8	867.9	407.3	537.47	**108.90**
	D	658.0	257.4	1883.6	428.9	502.79	**108.90**
SMAPE	A	**29.3**	106.3	59.9	33.7	31.75	42.67
	B	**28.9**	104.9	75.0	36.2	38.28	42.67
	C	**30.0**	99.1	50.1	33.8	33.44	42.67
	D	**29.3**	92.7	103.4	34.1	40.56	42.67

Global model errors (multiplied by 10-5) for extremely randomized trees (ET), gradient boosting (GB), multi-layer perceptron (MLP), random forest (RF), adaptive boosting (AB), and k-nearest neighbors (K-NN)

Geothermal Heat Exchanger Anomaly Detection Based on Virtual Sensors

Error	Experiment	ET	GB	MLP	RF	AB	K-NN
LMLS	A	2.9	15.7	1153.2	3.3	3.56	5.81
	B	3.2	19.5	77.7	3.9	3.96	5.81
	C	3.2	29.5	16.3	3.9	4.15	5.81
	D	3.1	34.1	304.7	4.0	3.73	5.81
MAE	A	232.0	689.1	3079.4	269.9	355.44	363.79
	B	255.1	832.2	1515.3	318.7	332.95	363.79
	C	280.8	1102.7	727.6	321.4	483.44	363.79
	D	278.4	1136.0	1675.1	320.7	407.91	363.79
MAPE	A	27.8	82.8	372.6	32.4	42.75	43.75
	B	30.6	100.2	183.2	38.3	40.00	43.75
	C	33.8	132.8	87.8	38.6	58.27	43.75
	D	33.5	136.8	202.6	38.5	49.10	43.75
MSE	A	5.9	31.5	3457.9	6.7	7.12	11.62
	B	6.3	39.0	157.5	7.8	7.93	11.62
	C	6.4	59.1	32.6	7.9	8.30	11.62
	D	6.2	68.3	672.6	8.0	7.45	11.62
NMSE	A	799.6	783.7	18418.0	544.7	724.68	98.50
	B	425.2	347.0	7103.5	366.3	731.76	98.50
	C	459.0	193.2	1652.2	361.8	111.51	98.50
	D	434.8	147.3	13330.6	408.	733.02	98.50
SMAPE	A	27.9	83.0	349.5	32.4	42.80	43.82
	B	30.7	100.4	184.3	38.3	40.05	43.82
	C	33.8	133.1	88.0	38.7	58.32	43.82
	D	33.5	137.1	198.0	38.6	49.15	43.82

Day model errors (multiplied by 10-5) for extremely randomized trees (ET), gradient boosting (GB), multi-layer perceptron (MLP), random forest (RF), adaptive boosting (AB), and k-nearest neighbors (K-NN)

Geothermal Heat Exchanger Anomaly Detection Based on Virtual Sensors

Error	Experiment	ET	GB	MLP	RF	AB	K-NN
LMLS	A	**0.05**	0.10	0.3	0.10	0.09	0.07
	B	**0.04**	0.10	3254.6	0.08	0.10	0.06
	C	**0.05**	0.10	0.10	0.07	0.09	0.06
	D	**0.04**	0.10	633.3	0.06	0.10	0.06
MAE	A	**38.6**	67.8	141.3	55.6	42.00	39.90
	B	**33.6**	57.6	14477.5	49.5	52.50	35.70
	C	**35.3**	65.1	110.6	48.1	42.00	37.80
	D	**33.3**	67.5	5595.9	45.9	52.50	37.80
MAPE	A	**4.7**	8.2	17.1	6.7	5.09	4.83
	B	**4.1**	7.0	1754.5	6.0	6.36	4.32
	C	**4.3**	7.9	13.4	5.8	5.09	4.58
	D	**4.0**	8.2	678.2	5.6	6.36	4.58
MSE	A	**0.11**	0.21	0.55	0.20	0.18	0.13
	B	**0.08**	0.21	6996.17	0.16	0.20	0.11
	C	**0.11**	0.20	0.20	0.14	0.18	0.12
	D	**0.08**	0.23	1291.10	0.13	0.20	0.12
NMSE	A	**4735.4**	8055.6	18847.7	7114.2	6805.56	822.22
	B	2407.6	**1427.0**	16796.8	5333.3	6388.89	1355.56
	C	**5349.2**	6283.4	22194.2	5732.9	6805.56	2355.56
	D	3829.9	7114.8	64166.1	**3324.2**	8055.56	2356.56
SMAPE	A	**4.7**	8.2	17.1	6.7	5.09	4.83
	B	**4.1**	7.0	1711.6	6.0	6.36	4.83
	C	**4.3**	7.9	13.4	5.8	5.09	4.83
	D	**4.0**	8.2	687.5	5.6	6.36	4.83

Night model errors (multiplied by 10-5) for extremely randomized trees (ET), gradient boosting (GB), multi-layer perceptron (MLP), random forest (RF), adaptive boosting (AB), and k-nearest neighbors (K-NN)

Geothermal Heat Exchanger Anomaly Detection Based on Virtual Sensors

- Conclusions
  - Anomaly detection is accomplished by measuring the deviation of the model with the real value of the S-315 temperature sensor.
  - For ranges greater than 2% the proposal has a nice performance.
  - It is possible both, the anomaly detection and the value recovery if it exist.

Grupo de Investigación
Ciencia y Técnica Cibernética

Máster Universitario en Eficiencia Energética y Sostenibilidad

Universidade da Coruña

Ciencia y Técnica Cibernética (CTC)

http://investigacion.udc.es/es/Research/Details/G00087